Baltic Sea Environment Proceedings
No. 94

Thematic Report

Validation of Algorithms for Chlorophyll *a* Retrieval from Satellite Data in the Baltic Sea Area

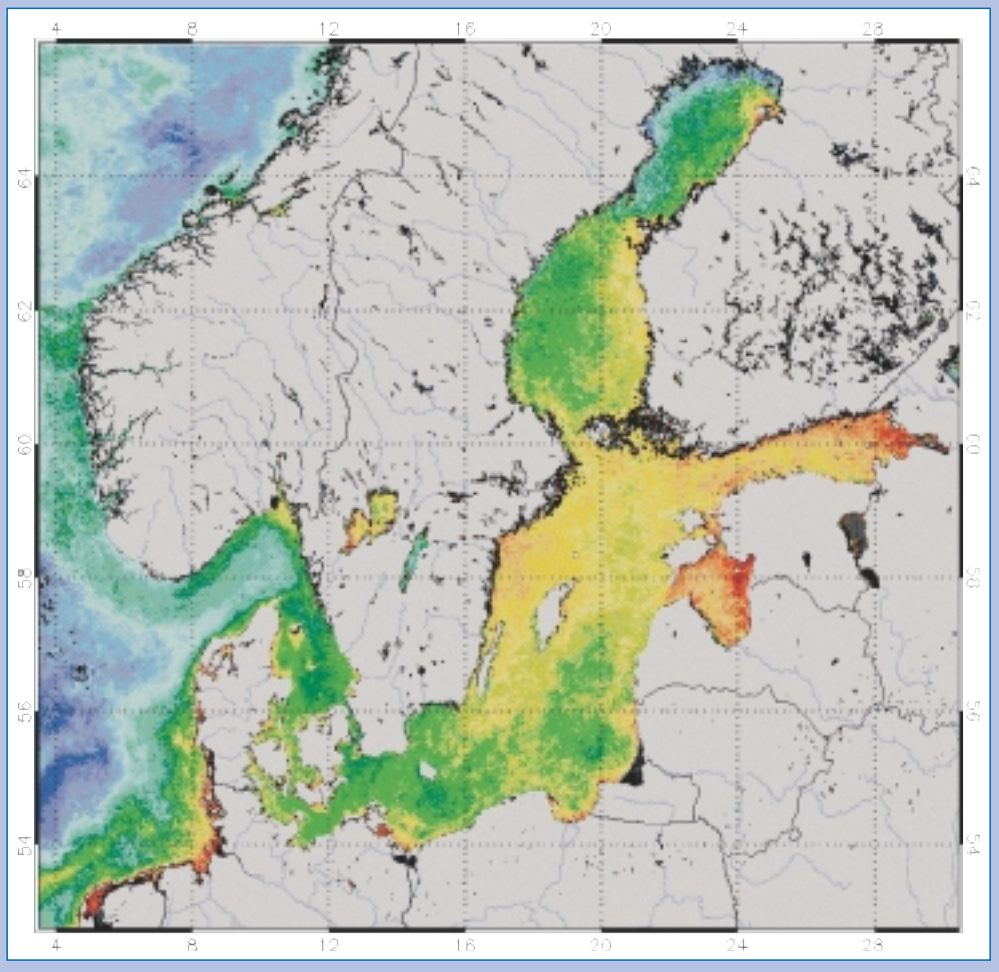

Helsinki Commission
Baltic Marine Environment Protection Commission

Baltic Sea Environment Proceedings

No. 94

Thematic Report

Validation of Algorithms for Chlorophyll *a* Retrieval from Satellite Data in the Baltic Sea Area

With contributions from:

Wolfram Schrimpf, (Project Co-ordinator), Jean-François Berthon, Barbara Bulgarelli, Davide D'Alimonte, Jean-Noël Druon, Frédéric Mélin, Giuseppe Zibordi
European Commission, JRC

Gunni Ærteberg Nielsen, Stiig Markager, Peter Stæhr - Denmark, NERI

Anu Reinart - Estonia, EMI

Sari Pertola, Eija Rantajärvi - Finland, FIMR, Kari Kallio, Jenni Vepsäläinen - Finland, FEI

Herbert Siegel - Germany, IOW

Juris Aigars - Latvia, IAE

Irina Olenina - Lithuania, CMR

Miroslaw Darecki - Poland, IO-PAS, Bogusz Piliczewski - Poland, IMGW

Bertil Håkansson - Sweden, SMHI,
Stefanie Hirch, Susanne Kratzer - Sweden, Stockholm University

Editor:

Wolfram Schrimpf - European Commission, JRC

Helsinki Commission
Baltic Marine Environment Protection Commission

2004

For bibliographic purposes this document should be cited as:
HELCOM, 2004
Thematic Report on Validation of Algorithms for Chlorophyll *a* Retrieval
from Satellite Data of the Baltic Sea Area

Baltic Sea Environ. Proc. No. 94

ISSN 0357-2994

Contents

Preface

Earth Observation satellite data provide a synoptic view of the physical and biological processes in coastal and marine ecosystems. So far this type of spatial information has not been used on a routine basis in HELCOM assessments. The European Commission's Joint Research Centre (EC/JRC) proposed the Project *Validation of algorithms for chlorophyll a retrieval from satellite data of the Baltic Sea area to* HELCOM MONAS 2/2001. The results of the Project should help to improve the use of information derived from Earth Observation data in the Baltic Sea area, in particular data derived from ocean colour. HELCOM MONAS 3/2001 approved the Project nominating EC/JRC as Project Coordinator and inviting all HELCOM Contracting Parties to participate actively.

The Project was officially launched with a kick-off meeting in Stockholm (31 January – 1 February 2002) organized by the Swedish Meteorological and Hydrological Institute / SMHI. All HELCOM Contracting Parties, except Russia, participated in the meeting. JRC supported the participation in the meeting by covering the travel expenses for one participant per HELCOM Contracting Party. The meeting defined the Objectives of the Project with the following key elements:

- To evaluate and assess current bio-optical algorithms for the retrieval of chlorophyll *a* from ocean colour data of the Baltic sea
- To exchange know-how, expertise and information between Project partners and participating institutions.

A second Project meeting was organized at JRC in Ispra, Italy (27-28 January 2003) with the aim of presenting and discussing the results obtained when carrying out the Project. All HELCOM Contracting Parties, except Germany and Russia, participated in this meeting. As for the kick-off meeting JRC supported the participation in the meeting by covering the travel expenses for one participant per HELCOM Contracting Party. The meeting also provided a forum for the participants to present their own research and development activities related to remote sensing in the Baltic.

The meeting concluded that a joint Final Report on the Project should be prepared that should address 1) in depth the evaluation of the present state of algorithms for chlorophyll *a* retrieval from satellite data of the Baltic Sea 2) the identification of gaps and next steps to further improve the use of satellite remote sensing of ocean colour in the Baltic and 3) the possibilities of how the collaboration of HELCOM institutions in the framework of this Project could be maintained and further developed in some kind of network activity.

The Draft Final Report was prepared by EC/JRC in cooperation with the participating institutions and presented at HELCOM MONAS 6/2003. The Meeting approved the Report and its publication in the *Baltic Sea Environment Proceedings*. The Final Report on hand was printed at the expense of EC/JRC.

Ispra, May 21st 2004

Wolfram Schrimpf
Project manager

Cover picture:
Concentration of chlorophyll *a* (mean July – August 2000) in the Baltic derived from SeaWiFS satellite data (OC4 algorithm); source: EC Joint Research Centre.

Abstract

The main Project task consisted of a comparison of the accuracy of three existing regional empirical algorithms for the computation of chlorophyll a *(Chl a)* from SeaWiFS (Sea-viewing Wide Field-of-view Sensor) images of the Baltic Sea. A fourth algorithm proposed for the production of global SeaWiFS *Chl a* products was also included as an additional element for comparisons.

The atmospheric correction scheme applied to the SeaWiFS imagery used in the inter comparison exercise relies on the coupling of an approximate radiative transfer model and the vicarious calibration of the space sensor. Because of the lack of *in situ* match-ups of normalized water leaving radiances, the accuracy analysis of the atmospheric correction scheme was restricted to the aerosol optical thickness. The results presented through scatter plots of SeaWiFS-derived versus in situ aerosol optical thickness at 443, 500, 670 and 865 nm, over 19 match-ups for the 2000-2001 period, show a determination coefficient always higher than 0.90, and a mean relative percentage difference ranging between 14% and 18% for the different channels.

The uncertainties in the *Chl a* determined with the 4 algorithms considered were assessed using *in situ* data of *Chl a* from stations and transects across the basin. The mean relative percentage differences between satellite derived and *in situ* values is quite large, ranging from 45 to 101% on optimal intercomparison conditions (i.e., with less than 5 hours time difference between in situ sampling and satellite overpass, and with an aggressive quality assurance of satellite data). An average underestimate of the satellite products with respect to the in situ concentrations is discerned, but no general bias is clearly observed. Relying on the results that present a comparison based on measurements collected in various months and locations by different research groups, it appears that none of the algorithms captures the overall variability of the chlorophyll concentration. The comparison gives slightly more encouraging results using match-ups obtained from separate Alg@line transects. In any case, it seems that the algorithms are not able to satisfactorily discriminate the spectral light contribution due to phytoplankton (and associate it with an actual pigment concentration) with respect to those due to the other optically significant components (i.e., dissolved organic matter and total suspended matter). Of the four algorithms, *OC4v4* shows the best results. Since it is an empirical algorithm whose formulation is heavily conditioned by data collected in open ocean waters, the statistical performance of *OC4v4* could be seen as fortuitous and resulting from a favorable functional form. On the other hand, it is worth remembering that the data that supported the development of the other regional algorithms are not necessarily highly representative of the spatial-temporal bio-optical variability of the entire basin, either because they are based on a limited number of points or because they are restricted to specific regional areas.

1. Project overview

W. Schrimpf, G. Zibordi
European Commission – Joint Research Centre
Institute for Environment and Sustainability – Inland and Marine Waters Unit
I-21020 Ispra (VA), Italy

1.1 Introduction and Objectives

Monitoring and assessment of the marine environment is the central focus of the activities of the HELCOM Monitoring and Assessment Group (HELCOM MONAS). In this context a major role of HELCOM MONAS consists in assessing the inputs of nutrients and hazardous substances and their effects in the marine environment. For this purpose HELCOM MONAS also co-ordinates national monitoring programmes and collects the resultant data. These environmental monitoring activities consist of examining various physical, chemical and biological variables. The relevant data is collected largely through in-situ campaigns and partly through the application of numerical models (atmospheric emissions and depositions).

So far spatial information derived from Earth observation satellite data has not been used on a routine basis in HELCOM assessments. A major reason why the use of this information is not yet 'widespread' could be the specific knowledge and know-how required to develop appropriate algorithms for the retrieval of the physical and/or biological variables over the whole basin and the processing and archiving of very large data volumes.

In January 1999 the Joint Research Centre (JRC) of the European Commission organized a Workshop on 'Satellite Observing Techniques as an Additional Research and Assessment Tool for Marine Inter-Regional Conventions' with the scope of presenting applications of satellite remote sensing for the marine environment and identifying the level of use and the needs of the Regional Marine Conventions for this kind of information in their monitoring and assessment activities. As an immediate follow-up of this workshop HELCOM invited JRC to present the use of Earth observation satellite data for monitoring and assessment of the marine environment at the joint TC INPUT and EC MON meeting Gothenborg, Sweden in April 1999. The Meeting invited JRC to present a proposal to HELCOM for a Project that should help to improve the use of information derived from Earth observation satellites, in particular from ocean colour.

The determination of *Chl a* from remote sensing data taken over the Baltic Sea presents considerable difficulties when compared to other European open and coastal waters. Major elements adding difficulties are the high sun zenith angles that make the atmospheric correction process critical, and the relatively high absorption of coloured dissolved organic matter that makes the application of universal *Chl a* algorithms less accurate. The rationale for the current Project was the need to investigate the accuracies of different algorithms specifically proposed for the determination of *Chl a* from satellite images of the Baltic Sea. The investigation carried out consisted in comparing in situ *Chl a* with those determined with different Baltic Sea algorithms applied to SeaWiFS atmospherically corrected data.

1.2 Summary of applied approach

The atmospheric correction of ocean colour data of the Baltic Sea is recognized to be a difficult task. A thorough analysis of the problem would require extensive investigations of the performance of different atmospheric correction codes and the availability of comprehensive and accurate match ups of atmospheric and marine radiometric data. However, recognizing that the exercise could not be carried out within the framework of this project due to the limited resources, one atmospheric correction code was adopted and its suitability for the Baltic Sea was checked prior to starting any algorithm comparison activity. The atmospheric correction code proposed for the activity, called REMBRANDT (Retrieval of Marine Biological Resources through Analysis of Ocean Colour Data), was developed at the JRC for SeaWiFS data processing (Bulgarelli and Mélin, 2000) and it is based on the scheme proposed by Sturm and Zibordi (2002), theoretically assessed by

Bulgarelli and Zibordi (2003) and successively updated by Mélin *et al.* (2003).

A simple assessment of the capabilities of the REMBRANDT code in accurately minimizing the atmospheric effects in SeaWiFS images of the Baltic Sea was carried out by comparing satellite derived and in-situ measured aerosol optical thickness.

Three algorithms for *Chl a* determination were considered for the intercomparison restricting the selection to those a) published and b) applicable to atmospherically corrected SeaWiFS imagery. The OC4V4 algorithm, applied by the SeaWiFS Project for global applications, was also added to the comparison analysis to ensure traceability of results with "standard" products. The comparison exercise was carried out using in situ *Chl a* and SeaWiFS data collected in the 2000-2001 time frame.

In the following chapters the selected Baltic Sea *Chl a* algorithms, the description and assessment of the REMBRANDT code for the Baltic Sea region, and the results of the algorithm inter-comparison, are presented in detail.

2. Chl *a* algorithms

F. Mélin, G. Zibordi
European Commission – Joint Research Centre
Institute for Environment and Sustainability – Inland and Marine Waters Unit
I-21020 Ispra (VA), Italy

2.1 Introduction

The Project aimed at assessing existing empirical algorithms for the computation of the chlorophyll *a* surface concentration from satellite images of the Baltic Sea provided by the Sea-viewing Wide Field-of-view Sensor (SeaWiFS, Hooker *et al.* 1992), making use of match-ups of in situ and atmospherically corrected remote sensing data. The atmospheric correction scheme adopted for the study is presented in Chapter 3.

An inventory of the Baltic Sea algorithms for pigment concentration computation led to the selection listed in the following section. The analysis was restricted to algorithms based on physical quantities produced by the atmospheric correction code (reflectance) and proposed for the SeaWiFS centre-wavelengths.

2.2 Algorithm inventory

The algorithms selected for the intercomparison are:

1. $Chl = 31.04893 \cdot (R_{510} / R_{670})^{-2.11508}$ proposed by Siegel *et al.* (1994);

2. $Chl = 4.21 \dfrac{(R_{510} / R_{555})^{-5.18}}{(R_{443} / R_{670})^{0.68}}$ proposed by Jørgensen and Berastegui (2000);

3. $Chl = 10^{[-0.141-2.8652 \cdot \log_{10}(R_{490} / R_{555})]}$ proposed by Darecki *et al.* (2002);

4. $Chl = 10^{[0.366-3.067R+1.930R^2+0.649R^3-1.532R^4]}$,

where $R = \log_{10}\left(\dfrac{\max(R_{443}, R_{490}, R_{510})}{R_{555}}\right)$ proposed by O'Reilly *et al.* (2000).

where R_λ indicates the remote sensing reflectance at centre-wavelength λ and *Chl* is either the chlorophyll *a* concentration or chlorophyll *a* + phaeopigment.

Algorithm 1 is based on 40 measurements distributed in the basin with an emphasis on the German Baltic coastal areas. The resulting empirical formula links optical field measurements and concentrations of chlorophyll *a* + phaeopigment.

Algorithm 2 used 28 SeaWiFS scenes matching measurement stations to derive a relationship between satellite reflectance and in situ chlorophyll concentrations collected in the North Sea, Skagerrak and western Baltic Sea (mostly Danish waters). No optical field measurements were available for the algorithm development. The satellite data were processed with SeaDAS version 4.0, with an added module for turbid water correction following Ruddick *et al.* (2000).

Algorithm 3 is based on field measurements of reflectance and chlorophyll a concentration (700 measurement stations) in the Southern Baltic (Polish coastal regions).

Algorithm 4, *OC4v4*, is added for comparison because it is the reference algorithm for global standard chlorophyll *a* SeaWiFS products. It is based on regressions performed on 2804 pairs of chlorophyll *a* concentrations and reflectance measurements distributed globally. Although its formulation was strongly influenced by measurements collected in open ocean waters, a significant part of the data was actually collected in shelf and coastal waters (but not in the Baltic area).

The first three algorithms are based on data collected in Baltic (or near-Baltic) waters. The four algorithms are empirical formula expressing chlorophyll *a* concentration as a function of various subsets of the SeaWiFS centre-wavelengths picked up between 443 and 670 nm. Corresponding satellite products are compared with field measurements of chlorophyll *a* concentration in Chapter 4.

3. Atmospheric correction of Sea WiFS data

B. Bulgarelli, F. Mélin, G. Zibordi

European Commission – Joint Research Centre
Institute for Environment and Sustainability – Inland and Marine Waters Unit
I-21020 Ispra (VA), Italy

3.1 Introduction

The Sea-viewing Wide-Field-of-view Sensor (SeaWiFS), a visible near-infrared multispectral scanner, has been providing the scientific community with a global coverage of the ocean since 1997. A processing tool was developed for the analysis of SeaWiFS imagery, making use of vicarious calibration to minimize uncertainties in absolute calibration and radiative transfer modelling of the atmospheric process. The developed software package is used to process SeaWiFS data from so-called Level-1A (raw data) to Level-3 (daily-to-monthly products over specified maps) over the European area. End products derived from SeaWiFS imagery are extensively used for the study of marine phytoplankton biomass distribution and production.

3.2 Description of the data processing scheme

The Level-1A data (i.e., raw data) received by all European receiving stations are obtained at GSFC DAAC (Goddard Space Flight Center – Data Active Archive Center) and all files are first merged into one file per satellite pass at LAC (Local Area Coverage) (high-) resolution. This step avoids any overlapping computation and is done once for all. Top-of-atmosphere Level-1A data are calibrated into Level-1B data.

The Level-2 calculation is based on the REMBRANDT code (Retrieval of Marine Biological Resources through Analysis of ocean colour DaTa), which provides standard products such as water-leaving radiance, aerosol optical thickness at 865 nm, chlorophyll *a* and sediment concentrations and diffuse attenuation coefficient. Ancillary data (atmospheric pressure, wind velocities and ozone load) are obtained from daily NCEP (National Center for Environmental Prediction) and TOMS (Total Ozone Mapping Spectrometer) files. The code uses the spectral characteristics of the top-of-atmosphere signal to classify the nature of the observed pixel (cloud, bright surface, vegetated surface, and water body). If the atmospheric correction and subsequent algorithms fail to derive physically sound information or if the obtained results fall outside the range of assumptions made to develop the algorithms, the pixel is flagged as a “bad value”. Level-2 output products are finally re-mapped onto geographical windows of interest and combined in time to yield Level-3 time series.

The calibration procedure and the atmospheric correction algorithm are briefly outlined below. An extensive presentation can be found in Sturm and Zibordi (2002), Bulgarelli and Zibordi (2003), Bulgarelli and Mélin (2000) and Mélin *et al.* (2002, 2003).

3.2.1 Calibration procedure

The calibration of SeaWiFS raw data into geophysical units is performed by removing the dark value (i.e., zero radiance), and applying a look-up table with absolute pre-launch calibration factors. A time-dependent correction, derived from lunar observations, is then utilized to compensate for the change of response with time for the various channels (Barnes *et al.* 2001).

Uncertainties induced in data processing by residual calibration uncertainty and non-accuracy in modelling the atmospheric radiative transfer processes, are minimized by multiplying the absolute calibration coefficients by vicarious adjustment factors $V_{cf}(\lambda)$. $V_{cf}(\lambda)$ were computed for the visible domain according to Sturm and Zibordi (2002) so as to minimize the difference between the normalized water-leaving radiance obtained from selected field measurements and that calculated from SeaWiFS calibrated data, processed with the atmospheric correction algorithm described below and subsequently corrected for spectral band-pass effects.

3.2.2 Atmospheric correction algorithm

Calibrated top-of-atmosphere SeaWiFS radiances are used to compute the radiance leaving the water surface by removing the atmospheric contribution to the total signal. Conditions of Sun glint are excluded with an appropriate flag. The model accounts for Rayleigh multiple scattering (scattering by atmospheric gas molecules), aerosol single scattering and Rayleigh-aerosol coupling through an iterative process.

The total radiance at the sensor $L_{tot}(\lambda_i)$, measured at centre-wavelength λ_i (for SeaWiFS: λ_1=412, λ_2=443, λ_3=490, λ_4=510, λ_5=555, λ_6=670, λ_7=765, λ_8=865 nm) is modelled according to

$$L_{tot}(\lambda_i) = L_{atm}(\lambda_i)+t(\lambda_i , \mu)L_w(\lambda_i) \quad (3.1)$$

with

$$L_{atm}(\lambda_i) = C_{ra}(\lambda_i)[L_a(\lambda_i)+L_R(\lambda_i)] \quad (3.2)$$

where $L_a(\lambda_i)$ and $L_R(\lambda_i)$ are the aerosol and Rayleigh radiances respectively, both accounting for specular reflection of the sea surface; $C_{ra}(\lambda_i)$ is the correction factor accounting for aerosol-Rayleigh interactions; $t(\lambda_i,m)$ is the atmospheric diffuse transmittance in the $\mu=\cos\theta_v$ direction, with θ_v the space sensor viewing angle and $L_w(\lambda_i)$ is the water-leaving radiance (the term that carries information on the seawater constituents). The Rayleigh radiance is taken from look-up tables and only depends on the Sun and sensor angles and the wind speed. With respect to the reference paper (Sturm and Zibordi 2002), Rayleigh radiance look-up tables are now taken from SeaDAS version 4 (Wang 2000). A turbid water correction is implemented to model the water leaving radiance contribution at wavelengths 765 and 865 nm (Mélin *et al.* 2003).

The atmospheric contribution for the bands 765 and 865 nm, directly computed from equations (3.1) and (3.2), is used to calculate aerosol radiance and optical thickness, and its value is extrapolated to shorter wavelengths.

The spectral variation of the aerosol radiance is modelled as

$$L_a(\lambda_i) = \varepsilon(\lambda_8,\lambda_i)L_a(\lambda_8)\frac{E_0(\lambda_i)}{E_0(\lambda_8)} \quad (3.3)$$

where $E_0(\lambda_i)$ is the solar irradiance attenuated by the ozone absorption and

$$\varepsilon(\lambda_8,\lambda_i) = e^{(\lambda_8-\lambda_i)} \quad (3.4)$$

The aerosol optical thickness is related to the aerosol radiance through a relationship in the single scattering approximation

$$\tau_a(\lambda_i) = \frac{4\pi\mu.L_a(\lambda_i)}{[p_a(\Psi_-)+[\rho(\mu)+\rho(\mu_0)]p_a(\Psi_+)]E_0(\lambda_i)} \quad i = 7,8 \quad (3.5)$$

where $p_a(\Psi)$ is the aerosol scattering phase function at Ψ; Ψ_- and Ψ_+ are the direct-solar-beam-to-sensor scattering angle and the reflected-solar-beam-to-sensor scattering angle respectively and $\rho(\mu)$ and $\rho(\mu_0)$ the Fresnel reflectances for flat sea surface in the μ and μ_0 directions.

The spectral dependence of the aerosol optical thickness is described by the Ångström law:

$$\tau_a(\lambda) = \alpha \cdot \lambda_i^{-\nu}, \quad i = 1,\cdots,6 \quad (3.6)$$

where α and ν are the Ångström coefficient and exponent, respectively. The correction process develops through nested iterations.

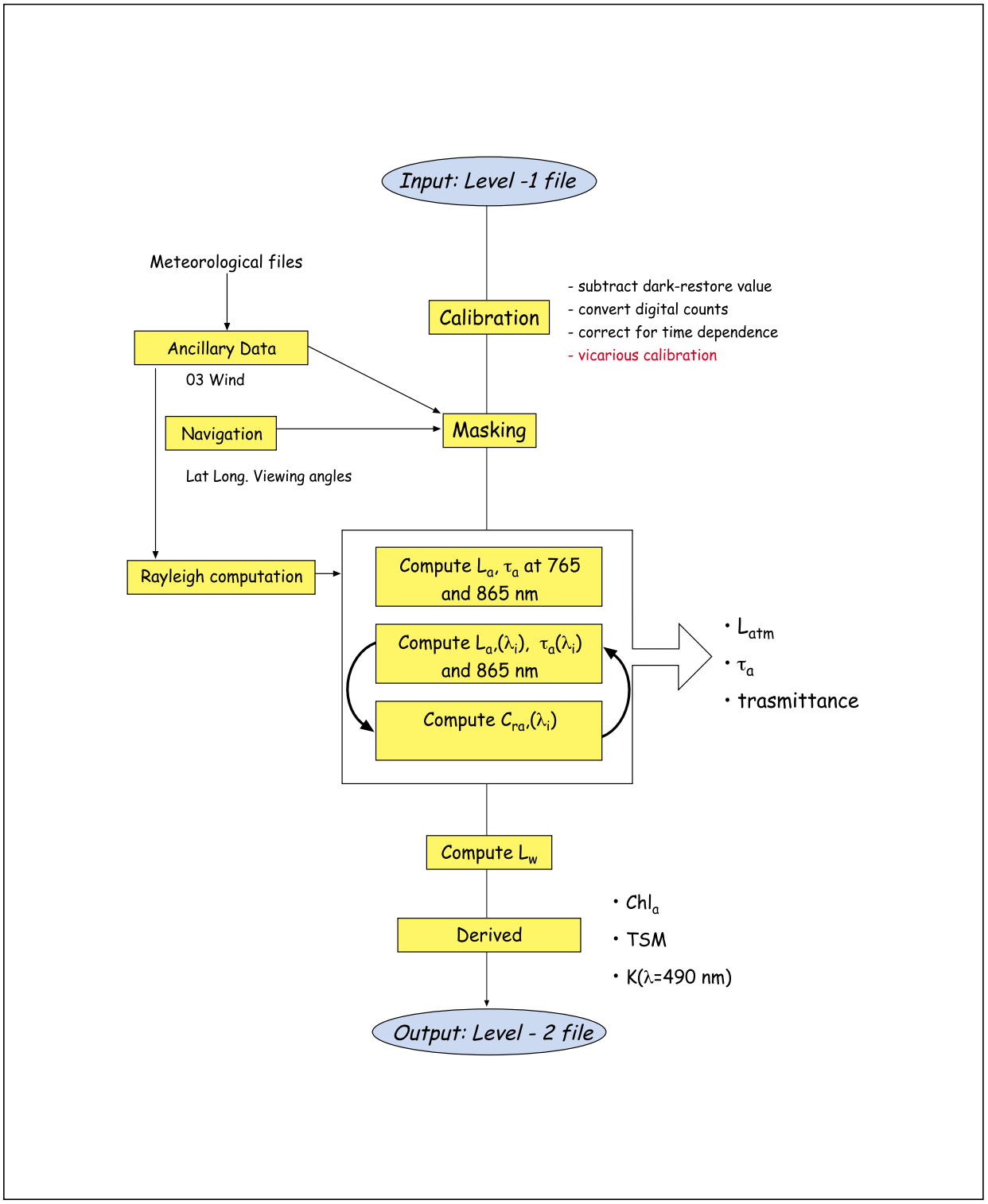

Fig. 3.1 Flow chart of the main-processing scheme.

3.3 Accuracy assessment

The relevance and the wide range of applications of SeaWiFS derived products underline the need for continuous and extensive effort in assessing and improving their accuracy. In order to fully support this objective, a theoretical evaluation of the accuracy of the atmospheric correction algorithm and a comparison between satellite-derived and in situ measured data was performed. The accuracy assessment was focused on the northern Adriatic Sea. Preliminary results were obtained for the Baltic Sea.

3.3.1 Accuracy assessment of atmospheric correction code

The accuracy of the atmospheric correction method included in the REMBRANDT processing scheme for SeaWiFS images was assessed for atmospheric and water parameters typical of midlatitude European sites, with specific reference to the northern Adriatic Sea. The main results are briefly summarized below. Detailed information can be found in Bulgarelli and Zibordi (2003), and Bulgarelli et al. (2002).

By using top-of-atmosphere radiance data simulated with the highly accurate FEM (Finite Element Method) radiative transfer code (Bulgarelli et al., 1999), the accuracy of the atmospheric correction method in the estimate of i) aerosol optical thickness, ii) water leaving radiance, and iii) remote sensing reflectance ratios was analysed at the SeaWiFS centre-wavelengths, accounting for seasonal variations in the Sun zenith. In addition a sensitivity analysis on noise sources in the NIR (Near Infrared) channels was also performed. Table 3.1 lists the geometric, marine and atmospheric parameters chosen as representative of the midlatitude

Satellite viewing angle θ_v	20° - 30° - 40° - 50°
Relative azimuth between sensor and Sun $\Delta\phi$	0° - 40°- 70°
Solar zenith angle θ_0	15° - 25° - 45° - 55°
Ångström exponent ν	1.4 -1.7 - 1.9
Ångström coefficient α	0.02 - 0.05 - 0.08
Aerosol single scattering albedo ω_{0a}	Maritime [(1)]
	Continental [(1)]
Chlorophyll *a* concentration *Chl [mg m^{-3}]*	0.3 - 3.0 - 10.0
Yellow substance absorption $a_{ys}(400)$ *[m^{-1}]*:	0.048 - 0.149 - 0.373

[(1)] *according to WMO 1984.*

Table 3.1
Geometric, atmospheric and marine parameters used in the accuracy assessment exercise.

Under the different simulated measurement conditions, the aerosol optical thickness at 865 nm, $\tau_a(\lambda_8)$, and the aerosol Ångström exponent ν are estimated with uncertainties lower than ±5% and ±8%, respectively, for 68% of the cases (Figure 3.2). The water leaving radiance is estimated with an accuracy that increases with Chl concentration (Figure 3.3). The accuracy is particularly low at 412 and 443 nm, because of large uncertainties in the atmospheric radiance computations due to a rough estimation of multiple scattering effects. Better results are obtained at wavelengths higher than 443 nm. In this region uncertainties exceed 10% for low Chl and a medium yellow substance absorption (i.e., $a_{ys}(400)=0.149 m^{-1}$) only.

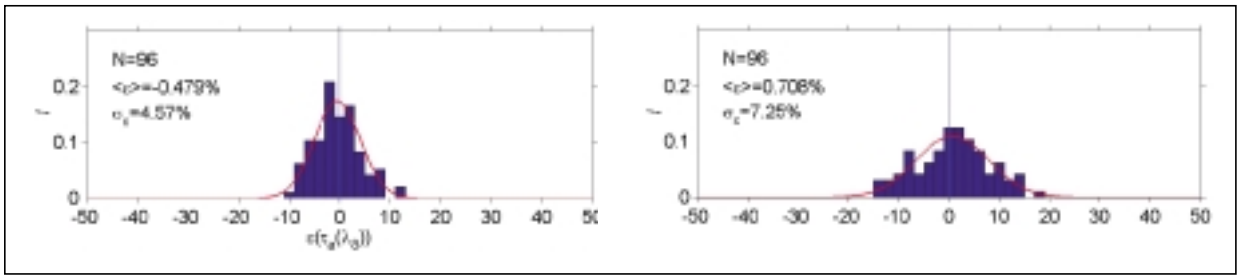

Fig. 3.2
Frequency histogram of the relative percentage difference ε between simulated and retrieved aerosol optical thickness $\tau_{\S}$ at λ_8=865 nm (upper panel) and the aerosol Ångström exponent ν (lower panel). *N* is the number of test cases, <ε> and σ_ε are the mean and standard deviations of the Gaussian fit.

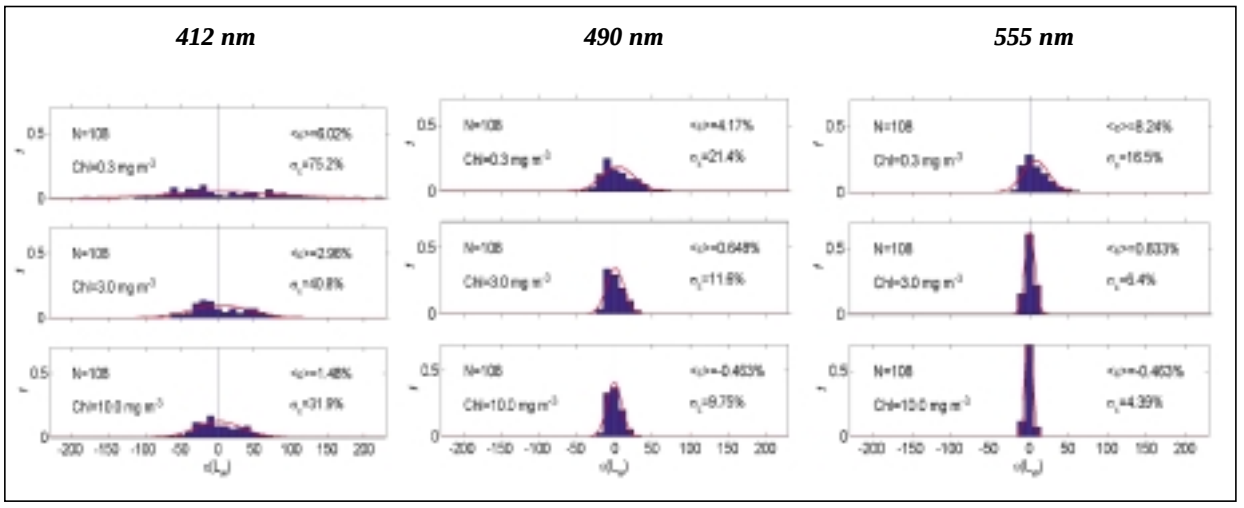

Fig. 3.3
Frequency histogram of the relative percentage difference ε between simulated and retrieved water-leaving radiance $L_w(\lambda)$ at 412, 490 and 555 nm, for $a_{ys}(400)=0.149$ m^{-1} and three different chlorophyll *a* concentrations.

The accuracy of the estimated water leaving radiance decreases with increasing $a_{ys}(\lambda)$. In agreement with an exponential decay of $a_{ys}(\lambda)$ with λ, the influence of $a_{ys}(\lambda)$ on L_w decreases as λ increases. Figure 3.4 shows the results obtained at 412 nm (the most affected wavelength). $\varepsilon(L_w)$ shows the highest sensitivity to $a_{ys}(\lambda)$ variations at low *Chl*. For each *Chl* value, the water signal decreases as $a_{ys}(\lambda)$ increases; correspondingly the scatter in ε, as characterized by the Gaussian standard deviation σ_ε, increases.

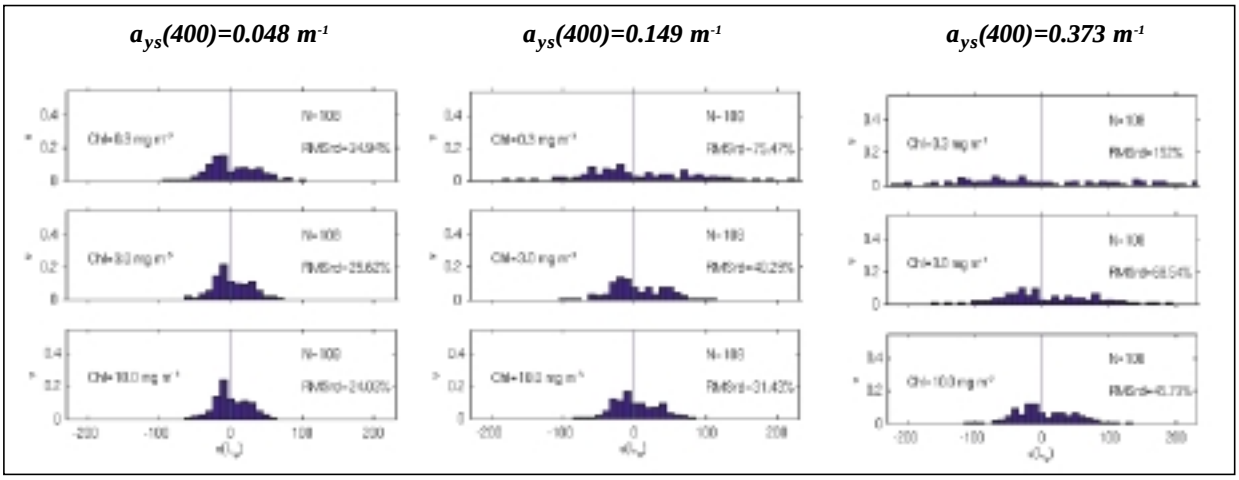

Fig. 3.4
Frequency histogram of the relative percentage difference ε between simulated and retrieved water-leaving radiance $L_w(\lambda)$ at 412 nm for $a_{ys}(400)$=0.048, 0.149 and 0.373 m^{-1} and three different chlorophyll *a* concentrations. *RMSrd* is the root mean square relative difference.

The Baltic Sea is characterized by $a_{ys}(\lambda)$ values which can be much higher than the values considered in the study described above. It is possible to foresee that increased yellow substance concentration will lead to a substantial decrease in the accuracy of the estimated water-leaving radiance in the blue part of the spectrum. Less sensitivity to $a_{ys}(\lambda)$ is found for wavelengths higher than 443 nm, especially for high chlorophyll a concentration. Figure 3.5 shows that the remote sensing reflectance band ratio R35 is estimated with an average uncertainty ranging between -5% (low *Chl* and $a_{ys}(\lambda)$) and 1% (high *Chl* and $a_{ys}(\lambda)$), and a standard deviation ranging between 3% and 7%, increasing as $a_{ys}(\lambda)$ increases. In the Baltic Sea, where even higher $a_{ys}(\lambda)$ values can be found, higher standard deviation values may be expected.

Keeping the same atmosphere-water conditions, it has been observed (Figures 3.6, 3.7 and 3.8) that the scheme is quite sensitive to seasonal changes in Sun zenith angle θ_0, tending to overestimate $\tau_a(\lambda_8)$, ν, $L_\omega(\lambda)$ and R_{35} for high θ_0 (i.e., in wintertime), and to underestimate them for low θ_0 (i.e., in summertime). Hence it is possible to foresee that, with the same atmosphere-water conditions, the scheme will tend to overestimate more in the Baltic region, characterized by high θ_0, than in the Adriatic region.

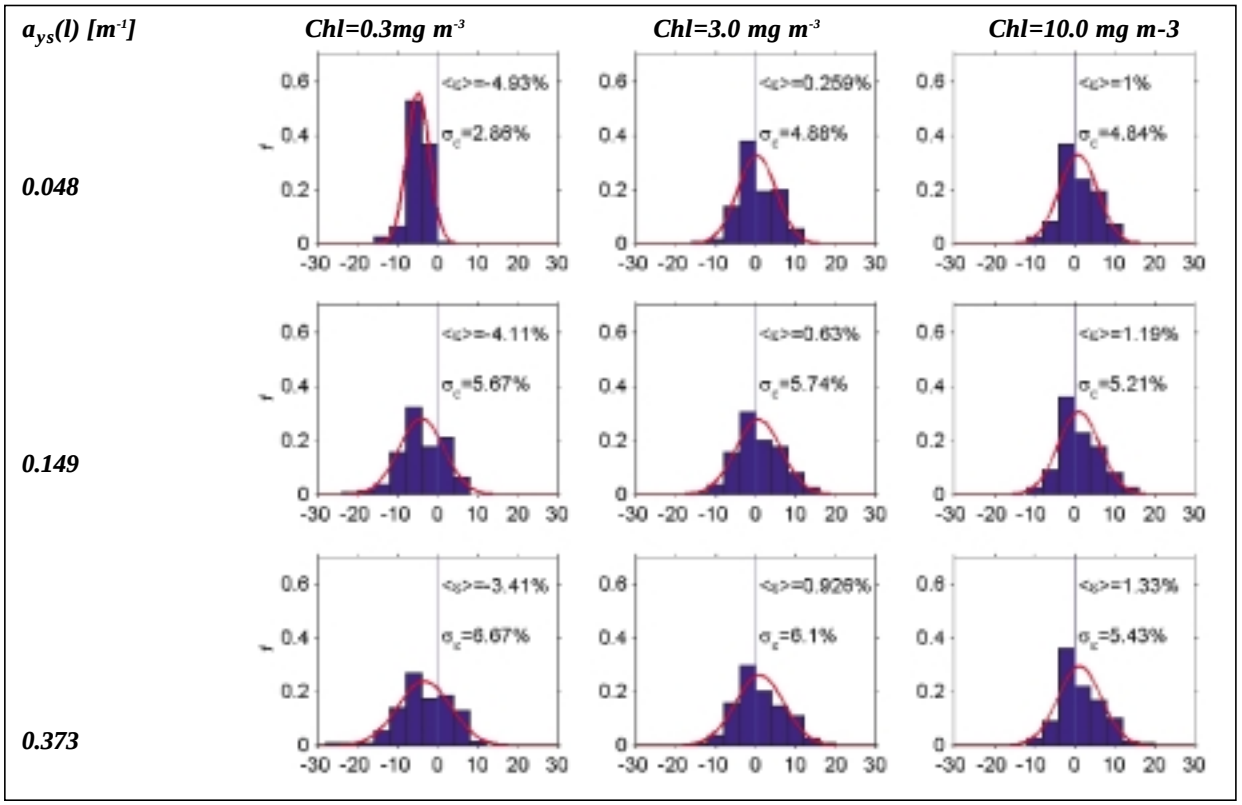

Fig. 3.5
Frequency histogram of the relative percentage difference ε between simulated and retrieved remote sensing band ratio R_{35} for different chlorophyll *a* concentrations and yellow substance absorption.

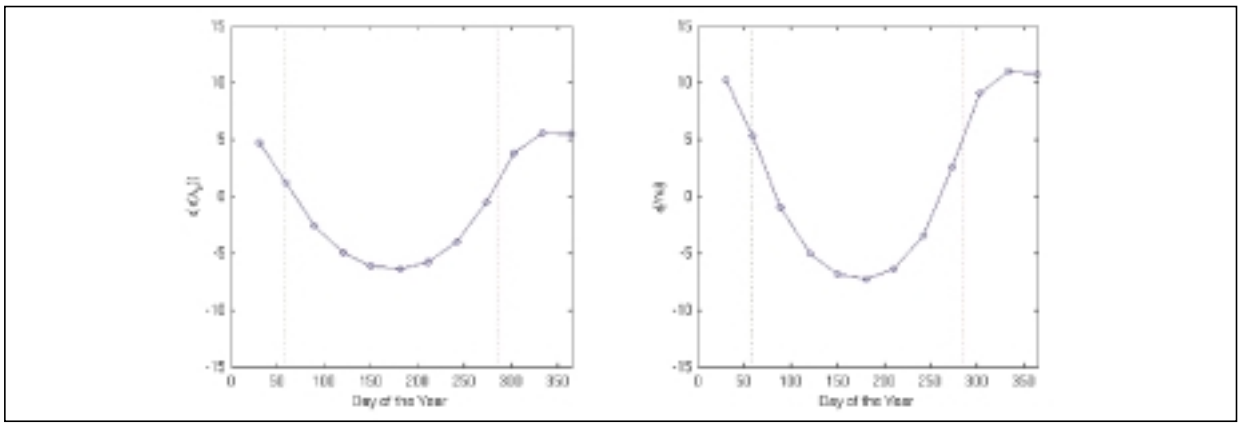

Fig. 3.6
Seasonal variation of $\varepsilon(\tau_a(\lambda_8=865\text{ nm}))$ and $\varepsilon(\nu)$ for a standard atmosphere (α=0.05, ν=1.7, maritime aerosol ω_{0a}), average viewing geometry (θ_v=25° and $\Delta\phi$=30°), mean yellow substance absorption ($a_{ys}(400)$=0.149 m^{-1}), and for a SeaWiFS overpass at about 12:00 GMT over the North Adriatic Sea (Lat. 45°18'50" N, Long. 12°30'30" E). The dotted lines delimit a region for which θ_0< 55°.

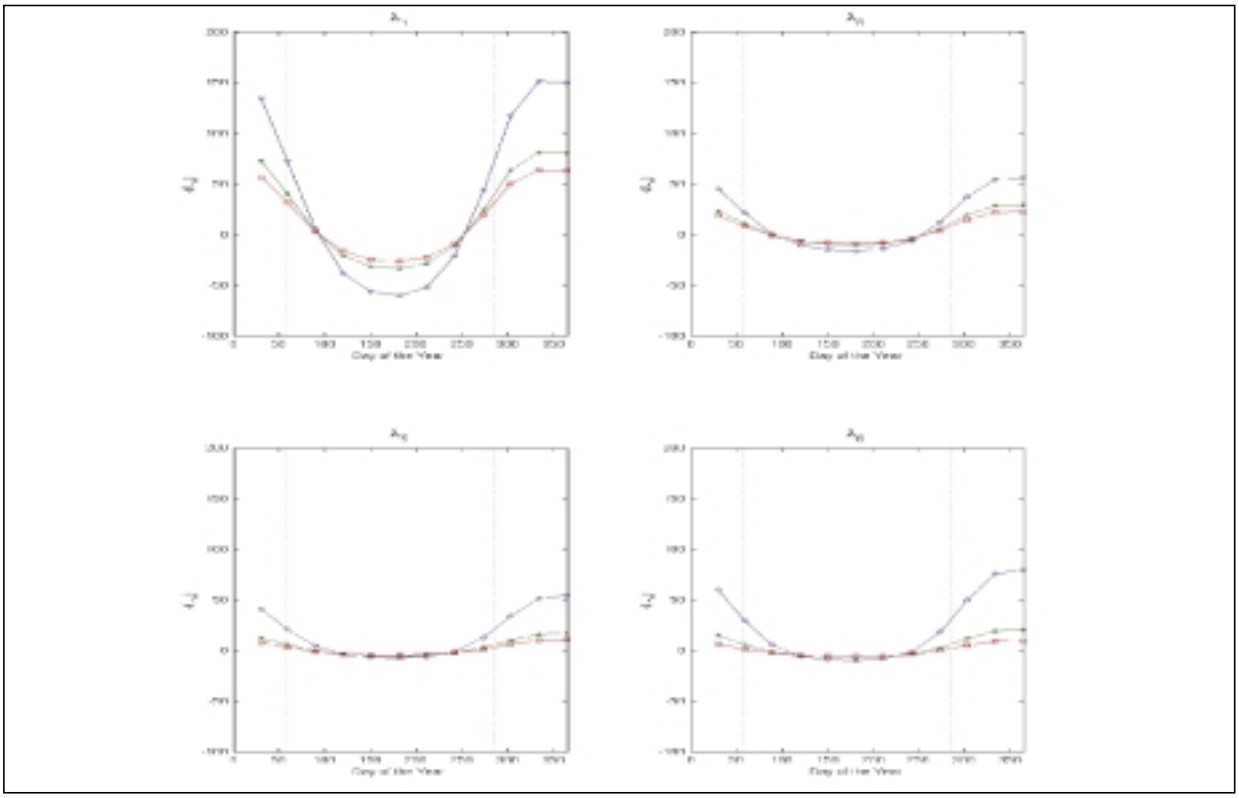

Fig. 3.7
Seasonal variation of ε(L_w) for (**o**)*Chl*=0.3 mg.m^{-3} , (*)*Chl*=3.0 mg.m^{-3} , (□)*Chl*=10.0 mg.m^{-3}. Data were produced under the same conditions as Figure 3.6 and for centre-wavelengths λ_1=412 nm, λ_3=490 nm , λ_5=555 nm , λ_6=670 nm.

The introduction of noise at 765 and 865 nm, accounting for signal-to-noise ratio and inexact prediction of the water-leaving radiance in the NIR, can lead to substantial uncertainties in the estimated ν and $L_w(\lambda)$ at 412-670 nm.

Results show that the coupling of an approximate atmospheric correction method with vicarious calibration of the space sensor is a valuable solution for the estimate of atmospheric and seawater parameters.
The results presented above are supported by the match-ups of *in situ* and SeaWiFS data for the period September 1997 – May 2002, presented in the following section.

3.3.2 Match-ups results

3.3.2.1 *AAOT (Acqua Alta Oceanographic Tower) site*

SeaWiFS primary products, obtained by applying the processing tool described in Chapter 3.2, were extensively validated with *in situ* data collected at the AAOT site (Figure 3.9) in the northern Adriatic Sea (Zibordi *et al.*, 2002). The validation was carried out through the analysis of match-ups covering the period September 1997 to September 2001. Some of the most significant results are presented below. An extensive analysis of the comparison between satellite-derived and *in situ* measured quantities, as well as the match-up protocol, is described in Mélin *et al.* (2003).

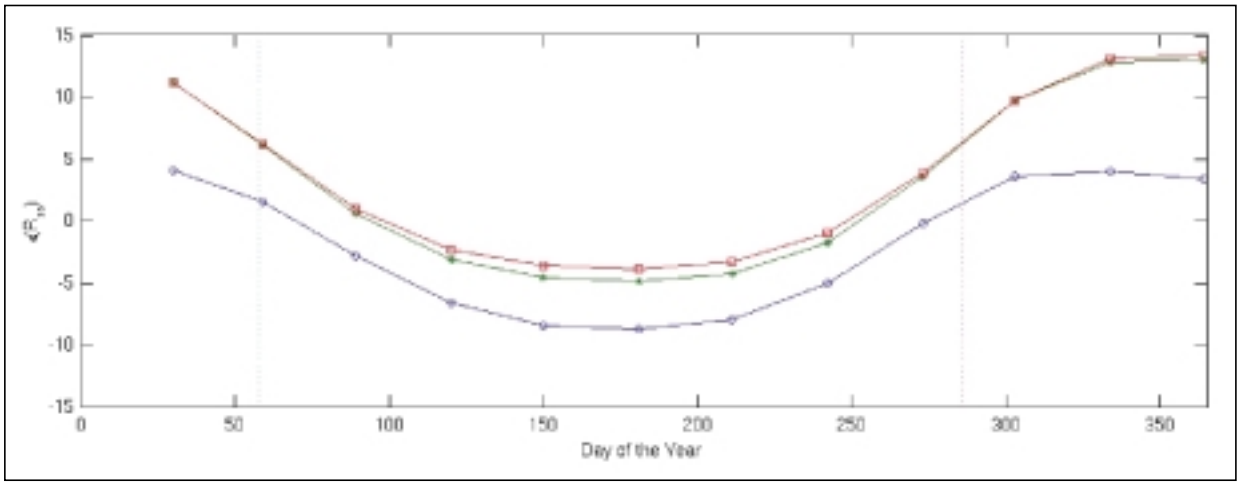

Fig. 3.8
Seasonal variation of ε(R_{35}) for (o)Chl=0.3 mg.m^{-3} , (*)*Chl*=3.0 mg.m^{-3} , (□)*Chl*=10.0 mg.m^{-3}. Data were produced under the same conditions as Figure 3.6.

Figure 3.10 displays the scatter plot of SeaWiFS-derived versus *in situ* aerosol optical thickness at 443 and 865 nm, over 197 match-ups.

The agreement between measured and satellite-derived aerosol optical thickness shows a determination coefficient r^2 ranging between 0.91 at 443 nm and 0.81 at 865 nm, and a mean relative percentage difference *d* (defined as the average ratio of the absolute difference of remotely sensed and *in situ* values divided by the *in situ* value, and expressed as percentage) ranging between 17% and 23% for the various channels.

Figure 3.11 shows the comparison between observed and remotely sensed normalized water leaving radiance for the different channels from 412 to 670 nm.

The determination coefficient r^2 is greater than 0.75 for the channels above 443 nm but decreases for the blue part of the spectrum. The mean relative percentage difference *d* is less than 20% for channels 490, 510 and 555, but as high as 47% and 29% at 412 nm and 443 nm, respectively. At 670 nm, the mean relative percentage difference d is 31%, with four satellite retrievals characterized by a very low normalized water- leaving radiance (below 0.2 mW cm^{-2} sr^{-1} nm^{-1}).

Fig. 3.9
The Acqua Alta Oceanographic Tower (AAOT) site in the northern Adriatic.

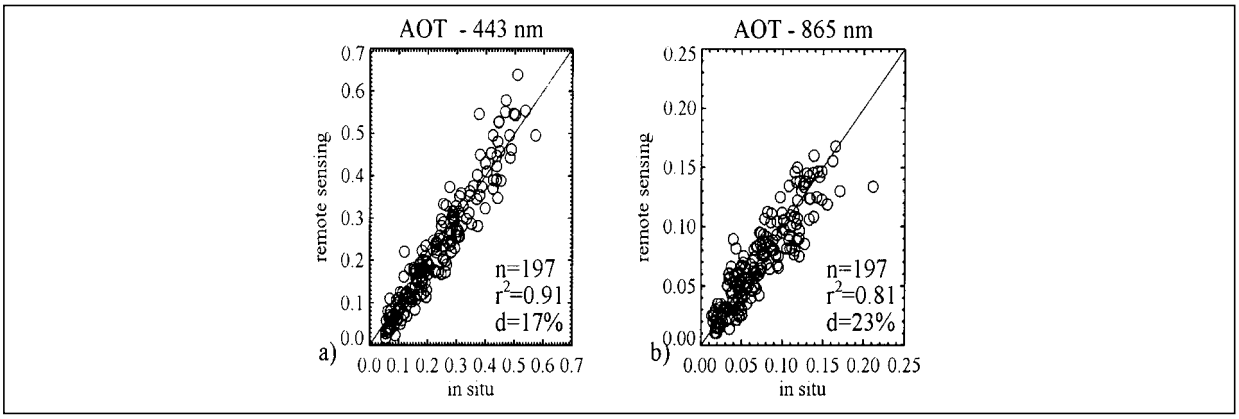

Fig. 3.10
AAOT site: scatter plot of SeaWiFS-derived versus in situ aerosol optical thickness (AOT) at 443 and 865 nm. *n* is the number of match-ups. r^2 is the coefficient of determination and *d* is the mean relative percentage difference.

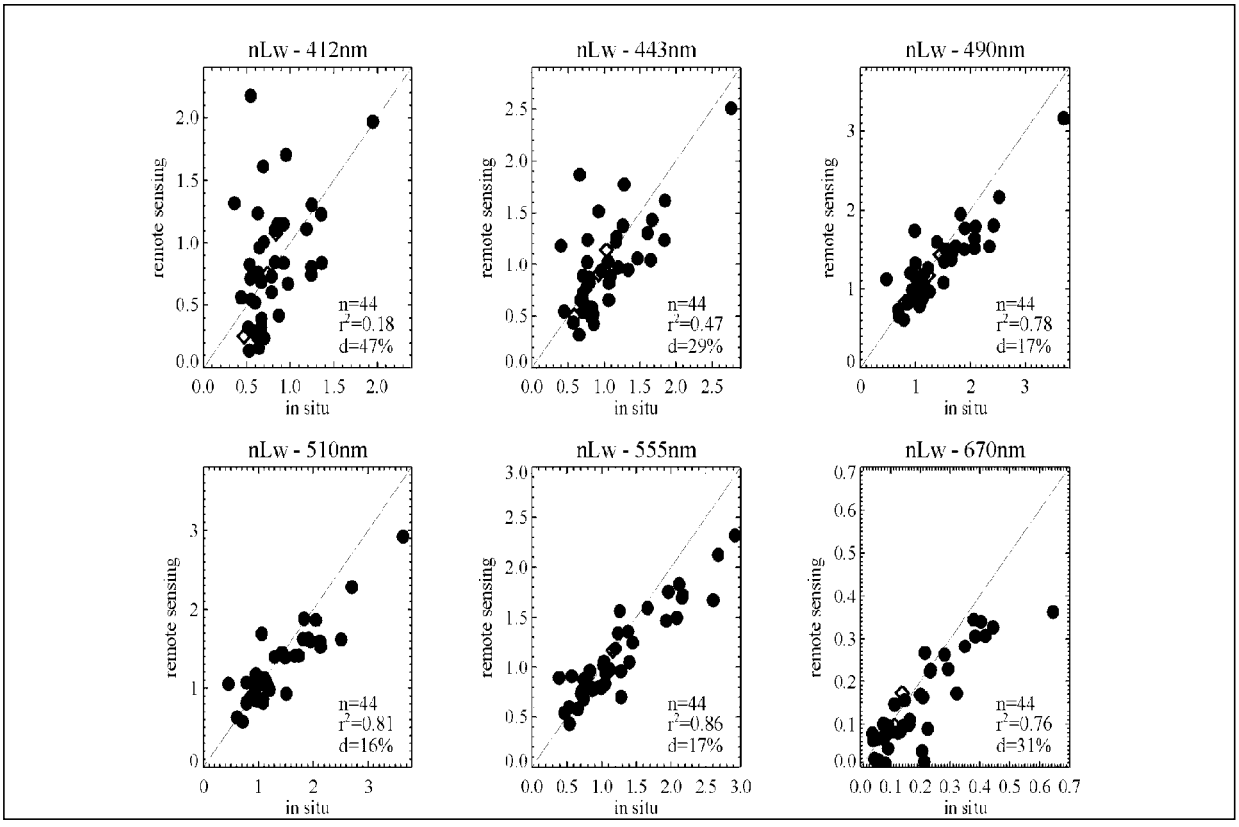

Fig. 3.11
AAOT site: scatter plot of SeaWiFS-derived versus in situ normalized water-leaving radiance nL_w for centre-wavelengths at 412, 443, 490, 510, 555 and 670 nm. *n* is the number of match-ups. r^2 is the coefficient of determination and d is the mean relative percentage difference.

3.3.2.1 Gotland site

The validation of the atmospheric correction code for the Baltic Sea is here restricted to aerosol products, since these are the only optical field measurements available for the study.

Aerosol *in situ* data were collected at the Gotland site (Figure 3.12), in the Baltic Sea, by B. Håkansson as part of the AERONET project.

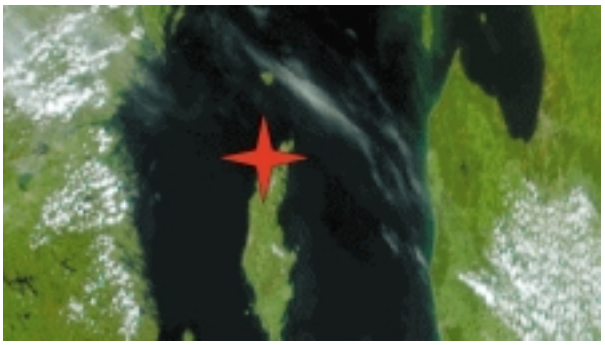

Fig. 3.12
The Gotland site in the Baltic Sea

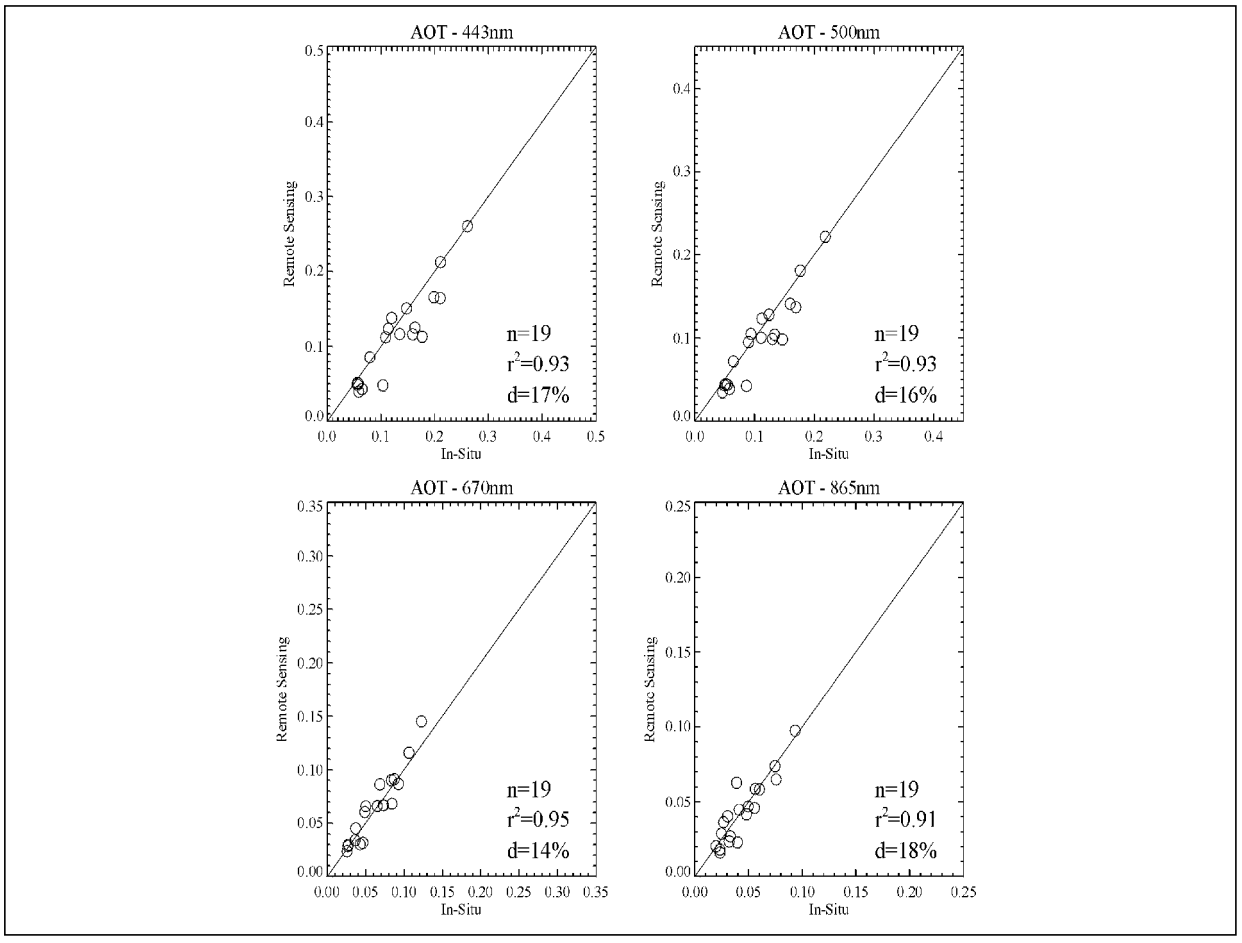

Fig. 3.13
Gotland site: scatter plot of SeaWiFS-derived versus in situ aerosol optical thickness (AOT) at 443, 500, 670 and 865 nm. *n* is the number of match-ups. r^2 is the coefficient of determination and *d* is the mean relative percentage difference.

The validation was carried out through the analysis of match-ups covering the period 2000-2001. The protocol of match-ups selection used in the case of the AAOT site was adapted. Indeed, the pixels closest to the measurement site and some surrounding pixels are land pixels (the site is located on the island) and cannot be included for the comparison. Instead, a large 21x21-pixel square centered on the measurement site is isolated. In that area considered representative of the aerosol conditions, the cloud-free 5x5-pixel square closest to the site is searched and serves for the comparison.
Figure 3.13 displays the scatter plot of SeaWiFS-derived versus *in situ* aerosol optical thickness at 443, 500, 670 and 865 nm, over 19 match-ups. The agreement between measured and satellite-derived aerosol optical thickness shows a determination coefficient r^2 always higher than 0.90, and a mean relative percentage difference d ranging between 14% and 18% for the different channels.

A more extensive validation of all SeaWiFS primary products relies on the availability of long-term accurate field measurements, including comprehensive atmospheric and marine data.

3.4 Conclusions for atmospheric correction

A processing tool was developed for the analysis of SeaWiFS imagery over the European area. The processing tool performs SeaWiFS atmospheric correction by coupling an approximate model and vicarious calibration.

The accuracy of the atmospheric correction scheme was theoretically assessed for atmospheric and water parameters typical of midlatitude European sites, with specific reference to the North Adriatic Sea. The atmospheric correction scheme showed an accuracy acceptable for environmental studies. The Baltic Sea is typically characterized by higher yellow substance absorption (e.g., in their review, Schwarz *et al.* (2002) indicate a mean $a_{ys}(440)$ of 0.41 m^{-1} with a standard deviation of 0.27 m^{-1}) and higher solar zenith angles. It is possible to foresee that the accuracy of the atmospheric correction scheme will not dramatically change in the retrieval of the aerosol optical thickness and the remote sensing band ratio, but it will greatly decrease in the retrieval of the water-leaving radiance in the blue part of the spectrum. A more detailed analysis should be carried out.
The accuracy of SeaWiFS derived primary products was evaluated by comparing satellite derived and *in situ* measured quantities. This validation activity has been extensively performed for the northern Adriatic Sea, where a comprehensive and highly accurate marine and atmospheric data set has been collected since 1995. The validation of the atmospheric correction code for the Baltic Sea has so far been limited to the aerosol products, since no other data set of optical properties was available for the project.

4. Algorithm comparison

F. Mélin
Inland and Marine Waters Unit, Institute for Environment and Sustainability,
Joint Research Centre, 21020 Ispra (VA), Italy

4.1. Introduction

This chapter describes the comparison of *in situ* data sets of chlorophyll *a* concentration with satellite-based products. First, the satellite data archive used for the comparison exercise is presented. It is based on products derived from the Sea-viewing Wide Field-of-view Sensor (SeaWiFS, Hooker *et al.* 1992). Then follows the comparison with the field measurements. This analysis was divided into two parts: one corresponds to a data body of chlorophyll a profiles distributed across the basin and collected in the years 1997-2001 by various Institutes. The second is a selection of chlorophyll *a* measurements for four transects across the basin.

4.2. Satellite products

The basis for the satellite data selection is the SeaWiFS ocean colour archive of the IMW Unit at JRC. This archive is organized into windows that cover the European seas and are displayed on http://www.me.sai.jrc.it. The Baltic window domain used here is shown on Figure 4.1 and is bounded by 52.75N – 66N in latitude and 3.5E – 30.5E in longitude. The projection is cylindrical equidistant with an approximate resolution of 2-km. The time series is organized in daily files as well as time composites, with 10-day and monthly periods. As indicated in Chapter 3, the atmospheric correction scheme is based on Sturm and Zibordi (2002). The operational aspects, including remapping and time binning techniques, are described in Mélin *et al.* (2000, 2002). One relevant aspect in the framework of this study is the limitation of the space sensor viewing angle at 45° (this threshold discards the pixels larger than 2-km in order to respect the resolution chosen for the grid).
The archive covers the period 1997-2001, but at present only the years 2000 and 2001 have been reprocessed with a revised atmospheric correction scheme (Sturm and Zibordi 2002, Mélin *et al.* 2003). To ensure a better quality of the satellite products used for the study as well as their consistency, only the time interval 2000-2001 is considered for the comparison.

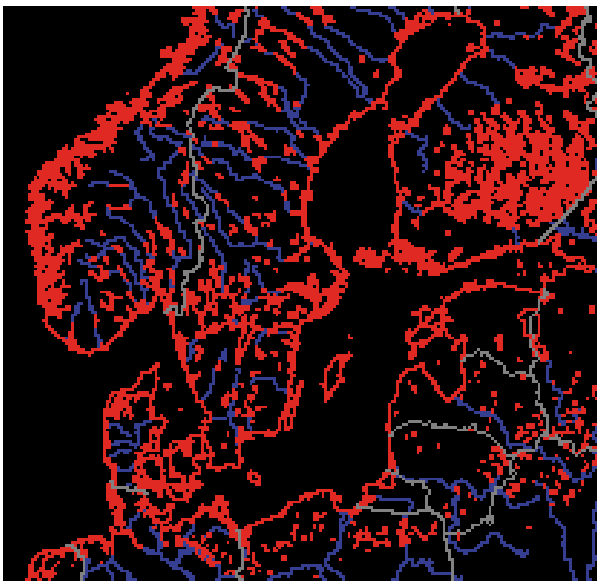

Fig. 4.1
Baltic window domain: latitude 52.75N – 66N, longitude 3.5E – 30.5E.

For each measurement, the archive is searched for the appropriate day and location and the relevant products (including top-of-atmosphere radiance, aerosol characteristics, normalized water-leaving radiance, geometry of illumination and observation) are extracted for comparison with the field value. The extraction includes a 3x3-grid point square centered on the element closest to the measurement. For the grid points associated with a valid normalized water leaving radiance spectrum nL_w, the chlorophyll *a* concentration is computed for the 4 algorithms considered for the comparison exercise (see Chapter 2); the average and standard deviation over the valid points are then calculated. The results of the 4 algorithms will be designated as *c1* (Siegel *et al.* 1994), *c2* (Jørgensen and Berastegui, 2000), *c3* (Darecki *et al.* 2002) and *OC4v4* (O'Reilly *et al.* 2000).

Following criteria on the number of valid points over the 3x3-grid and the conditions of satellite observation (see below for the actual conditions), a number n of match-ups (coincident satellite value and field data) is selected. The following indices of comparison between measurements m and satellite values s of the chlorophyll a concentration are then used:

$$rmsrd(m,s) = \sqrt{\frac{1}{n}\sum_{i=1}^{n}\left(\frac{s_i - m_i}{m_i}\right)^2}$$

$$rms\ \log(m,s) = \sqrt{\frac{1}{n}\sum_{i=1}^{n}(\log_{10} s_i - \log_{10} m_i)^2}$$

$$mrd(m,s) = \frac{1}{n}\sum_{i=1}^{n}\frac{|s_i - m_i|}{m_i}$$

$$md(m,s) = \frac{1}{n}\sum_{i=1}^{n}\frac{s_i - m_i}{m_i}$$

rmsrd and *mrd* are the root mean square relative difference and mean relative difference, respectively. These indicators are more sensitive to overestimates of m by s than to underestimates. On the other hand, *rms*log gives equal weight to an underestimate by a given factor and to an overestimate by the same factor. *md* is an unsigned difference that quantifies a systematic bias between m and s. r^2 is the coefficient of determination.

4.3. Basin scale field data and comparison with satellite products

4.3.1 Description of the field data sets

A pool of data was provided through the International Council for the Exploration of the Sea (ICES). This compilation of data sets collected by various Institutes contains 1124 chlorophyll a concentration profiles of variable depth distributed across the basin for the period 1997-2001. An additional data body was provided directly by the Swedish Meteorological and Hydrological Institute (SMHI, B. Håkansson). It contains 2119 chlorophyll *a* profiles, geographically widely distributed but with an emphasis on the Swedish coastal waters. 593 of those profiles were already in the ICES database and were therefore not taken into account as additional information. Table 4.1 shows the number of profiles per season and per year for the resulting ensemble of 2750 profiles, and Figure 4.2 gives the geographical distribution of the data points pooled per season. Only the surface or near-surface concentration is used in this study for comparison with the satellite counterpart.

N. Profiles	1997	1998	1999	2000	2001	ALL
DJF	59	130	120	125	109	582
MAM	110	122	124	150	103	609
JJA	172	162	227	210	125	896
SON	142	150	130	151	90	663
ALL	483	564	601	636	427	2750

Table 4.1
Number of profiles per season and per year. DJF: Dec. (of the year before)-Jan.-Feb., MAM: Mar.-Apr.-May, JJA: Jun.-Jul.-Aug., SON: Sep.-Oct.-Nov.

The seasonal distribution is fairly even. However, many data points are located very close to the coast. It has already been pointed out that the possibility of comparing remote sensing ocean colour products to very coastal field measurements is expected to be low. Furthermore satellite ocean colour provides insufficient coverage for the winter season (i.e., December to February).

No comprehensive description of the data collection (technique used, expected accuracy) was available for this activity. An index of the repeatability of the measurements, including the natural variability and local heterogeneity, can be inferred from the presence in the data set of 197 replicates, i.e., multiple values (2 to 4) of chlorophyll *a* concentrations at the same depth for the same profile. The ratio of the standard deviation calculated for these multiple values over their mean value was less than 10% for 121 replicates. This ratio was between 10% and 25% for 50 replicates and above 25% for 21.

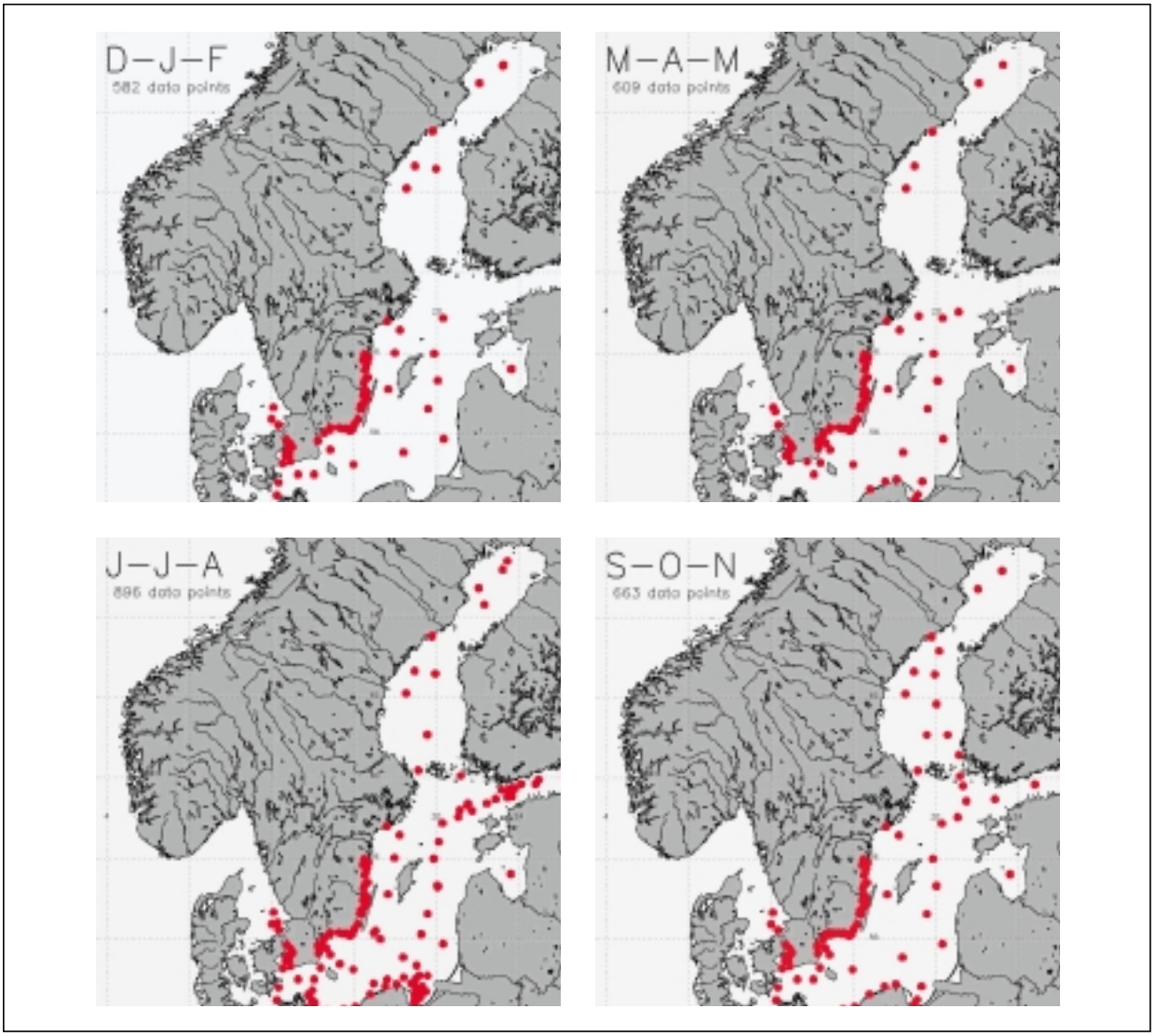

Fig. 4.2
Seasonal and spatial distribution of the 2750 chlorophyll *a* profiles.

With the availability of this large data set, widely distributed in space and time, one can obtain a broad view of the basin biomass variability, for instance in terms of seasonal cycle. Figure 4.3 shows an example of a seasonal cycle for the year 2000. All points available for a season were pooled together for a plot making use of a contouring graphical tool. This example provides more information about the spatio-temporal variability characterizing the Baltic domain. Values indicated by the contours may be safely considered when close to the measurement points but great caution is required in between.

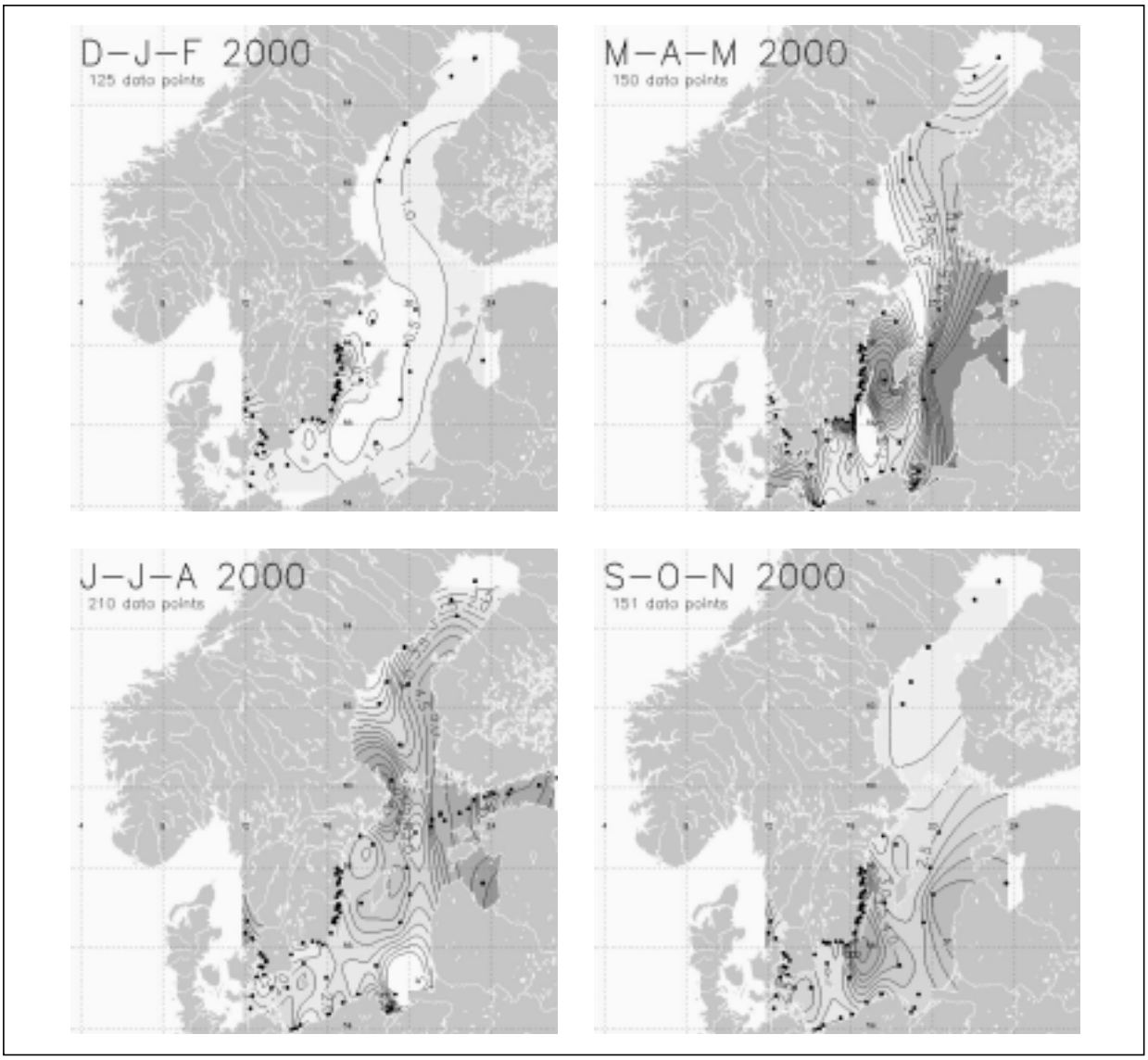

Fig. 4.3
Chlorophyll *a* seasonal cycle for 2000. The field measurements available for a given season are pooled together and serve as input to a contouring procedure.

The Baltic Sea is obviously characterized by elevated levels of biomass. Some abnormal features for spring (Mar.-May) might result from rapid changes taking place at this time of the year. The trend is towards slowly decreasing concentrations in summer and autumn. An increasing gradient of concentrations is apparent towards the eastern coasts of the Gulf of Riga and the Gulf of Finland, as well as in the Gulf of Bothnia proper. Not surprisingly, a northward negative gradient can also be noticed. This is not the place to give a complete description of the spatio-temporal variability of phytoplankton in the Baltic, but the features outlined on the basis of Figure 4.3 correspond to common knowledge for the area. Low values are only typical of wintertime and the summer minimum. During the spring period (Mar.-May) the phytoplankton biomass increases rapidly in a few weeks and has its highest values for the whole year. After the spring bloom, the algal biomass decreases to a short summer minimum. With the increasing surface water temperatures, the amount of cyanobacteria increases and blooms with large areal coverage can occur. Later in the autumn, some local blooms of diatoms might develop, but in general the amount of algae decreases towards the winter while availability of light diminishes.

After the description of the *in situ* data sets, the results of the comparison with satellite products are presented.

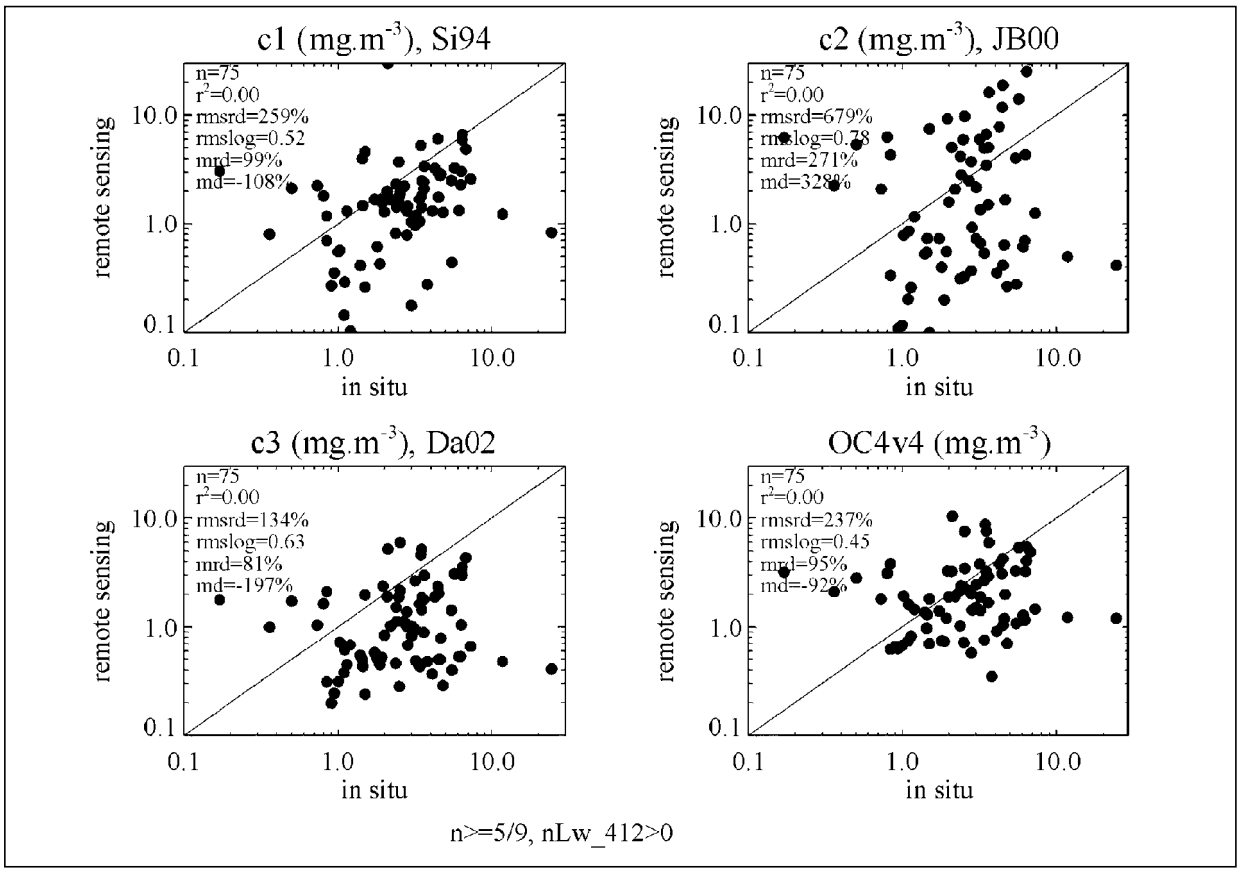

Fig. 4.4
Match-ups between satellite derived and *in situ* chlorophyll *a* concentrations. The minimum number of valid points in the 3x3-grid point square centered on the measurement site is set to 5. *n* is the number of match-ups and the other variables were introduced in Section 4.2.

4.3.2 Match-ups analysis

If the threshold of the minimum number of complete normalized water leaving radiance spectra nL_w (from 412 to 670 nm) over the 3x3-grid point square is set to 5 (i.e., at least half the points in the square have yielded valid values), the number of match-ups equals 75 (Figure 4.4) with field values spanning 2 orders of magnitude. Except for *c2*, the satellite derived concentrations tend to be lower than the field values. For all 4 algorithms, the dispersion of points is huge and the coefficient of determination is virtually null. *rms*log values indicate that the mean difference between *in situ* and remote sensing concentrations is at least half an order of magnitude.

A number of valid points in the 3x3-grid point square strictly less than 9 is indicative of conditions not favorable for the atmospheric correction scheme (e.g, vicinity of a cloud, failure of the atmospheric correction scheme in presence of a turbid atmosphere and / or water, bottom effect). A threshold of the minimum number of complete nL_w spectra over the 3x3-grid point square equal to 9 (i.e., all the points in the square have yielded valid values) improves the validity of the comparison. The remaining 37 match-ups are presented on Figure 4.5. No statistical improvement is noticed.

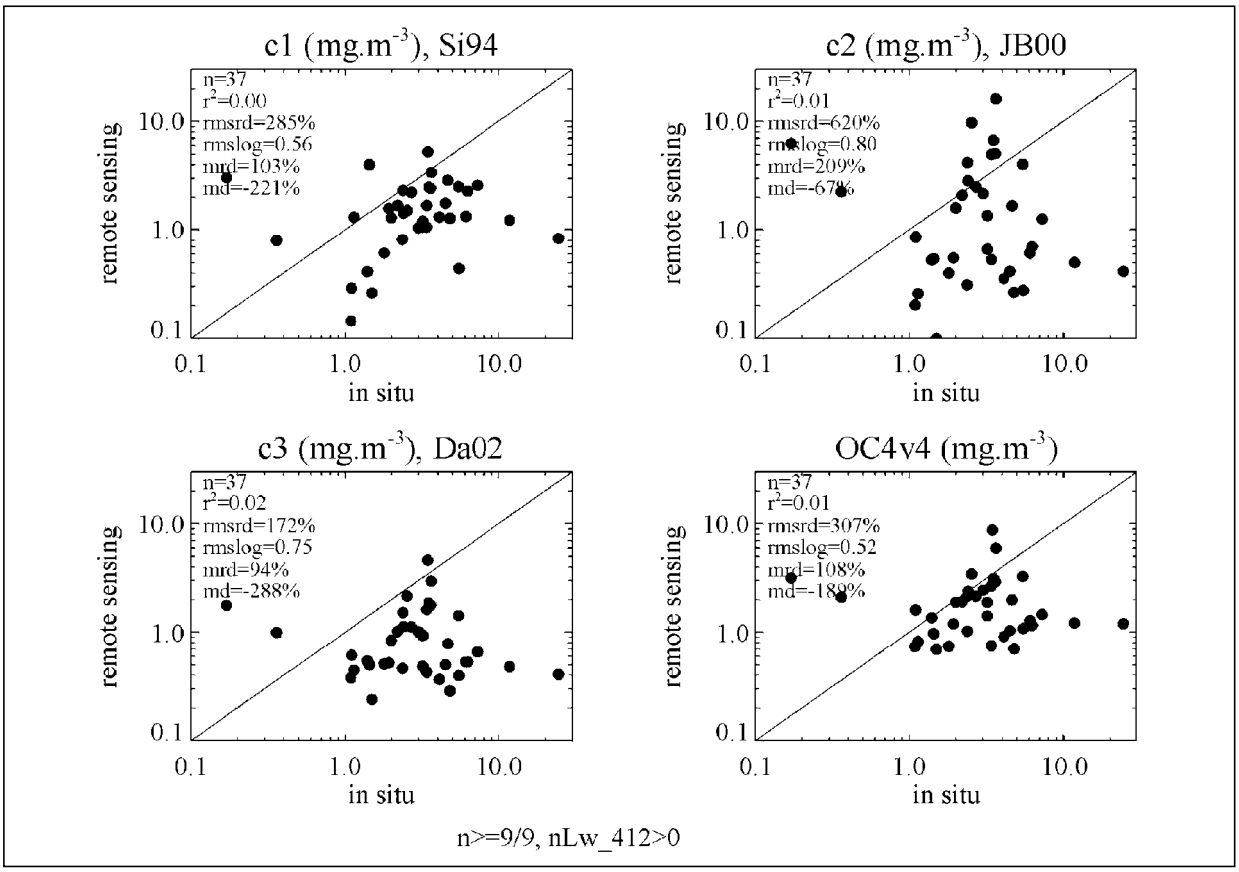

Fig. 4.5
Match-ups between satellite derived and *in situ* chlorophyll *a* concentrations. The number of valid points in the 3x3-grid point square centered on the measurement site is set to 9. *n* is the number of match-ups and the other variables were introduced in Section 4.2.

The only time constraint applied so far for the selection of the match-ups between the two types of measurements was their occurrence on the same day. However, some measurements were collected in early morning or late afternoon and evening, and this large time difference with the satellite overpass (around local noon) might alter the comparison in cases of strong variability. Figure 4.6 shows the match-ups (15) left if the difference between measurement and satellite pass is restricted to 5 hours.

The overall trend is an underestimate of the field measurements by the remote sensing values. The mean relative difference is 63%, 101%, 65% and 45% for *c1*, *c2*, *c3* and *OC4v4* respectively. This improvement is not accompanied by a larger coefficient of determination that is still not significantly different from 0.

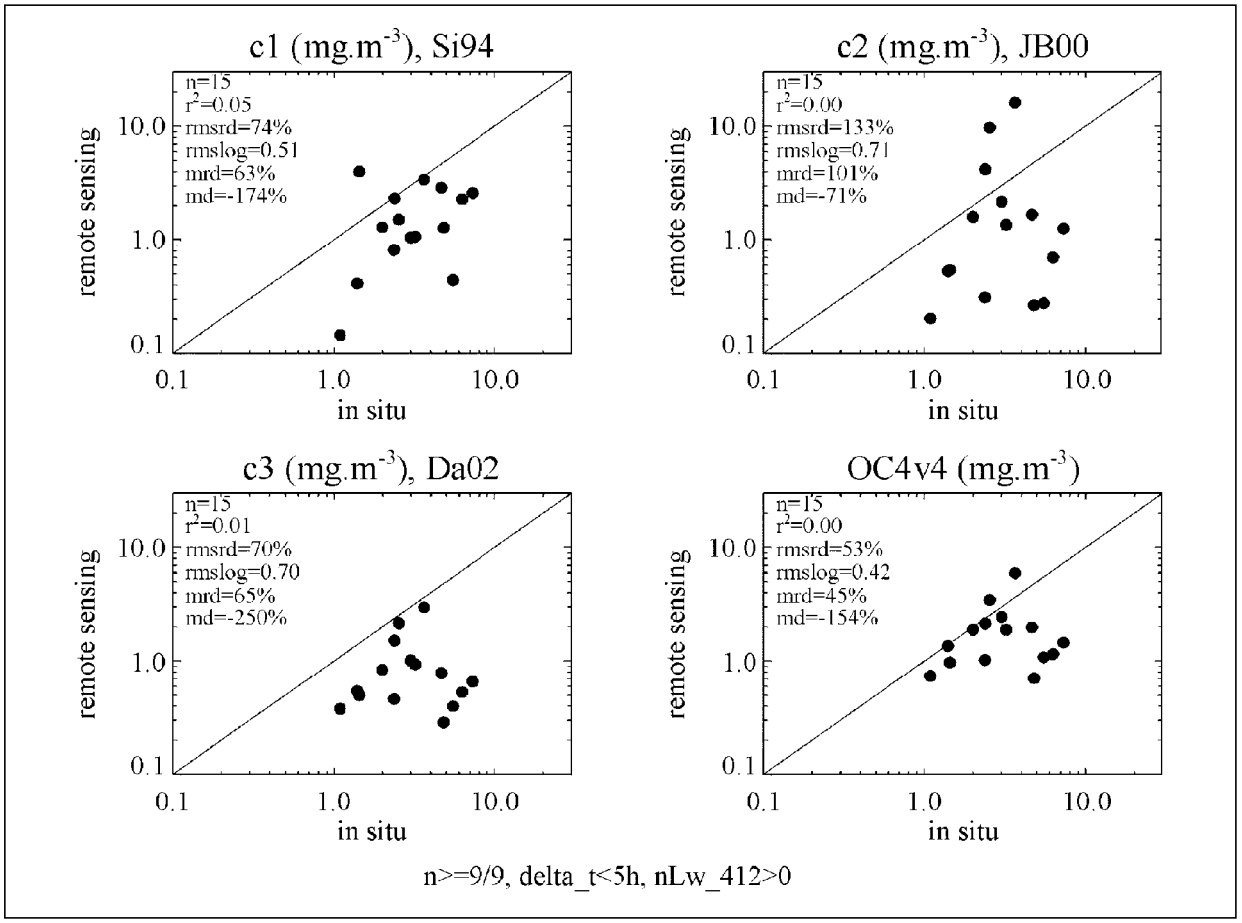

Fig. 4.6
Match-ups between satellite derived and *in situ* chlorophyll *a* concentrations. The number of valid points in the 3x3-grid point square centered on the measurement site is set to 9. The time of measurement is within +/- 5 hours of the satellite overpass. *n* is the number of match-ups and the other variables were introduced in Section 4.2.

The inputs to the algorithms rely on various sets of channels and there is no simple analytical relationship linking the algorithm outputs. In order to gain a better sensitivity on the respective algorithm outputs, each one is compared on Figure 4.7 to the average of the four algorithms for the 37 match-ups of Figure 4.5 (here, the time of measurement is not an issue). Since all algorithm output are *a priori* valid, this comparison is also a conservative estimate of the algorithm uncertainties. *OC4v4* is the most representative of the mean of the 4 algorithms. The distribution associated to c1 is also close to the mean but with more scatter. *c2* provides values that are relatively higher in the high concentration range and lower in the low range. c3 tends to be relatively lower than the other algorithms. Overall, the four algorithms yield comparable estimates: the mean relative difference (*mrd*) with respect to the average is below 50%. Since those algorithms rely on a varied set of nL_w channels, ranging from 443 to 670 nm, and the results presented are for a limited number of points, the respective behaviour of the 4 algorithms as displayed on Figure 4.7 should not lead to any general conclusion as to their application to the entire basin.

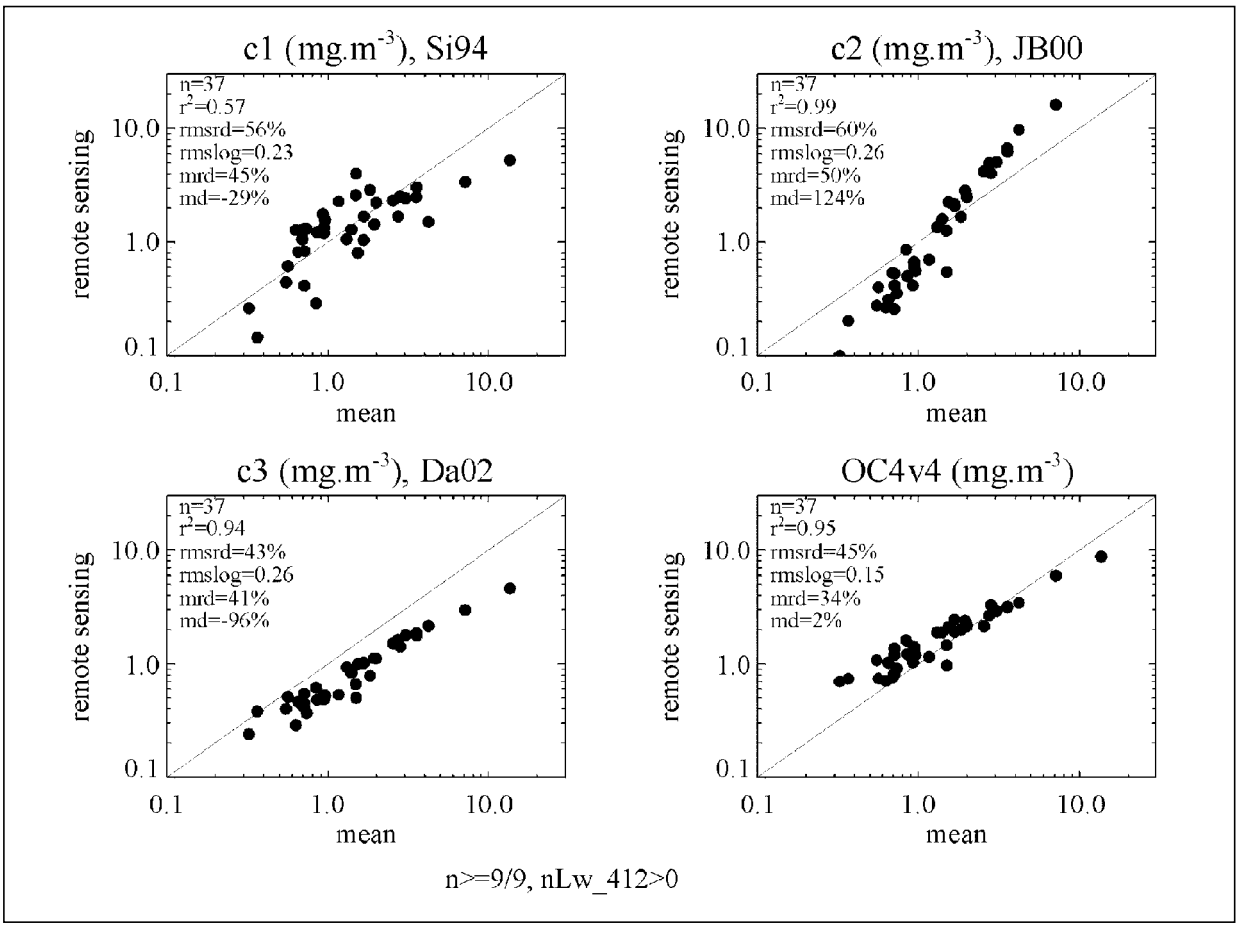

Fig. 4.7
For the match-ups displayed on Figure 4.5, scatter plots of each algorithm with respect to the average of the 4 algorithms (*c1+c2+c3+OC4v4*) / 4.

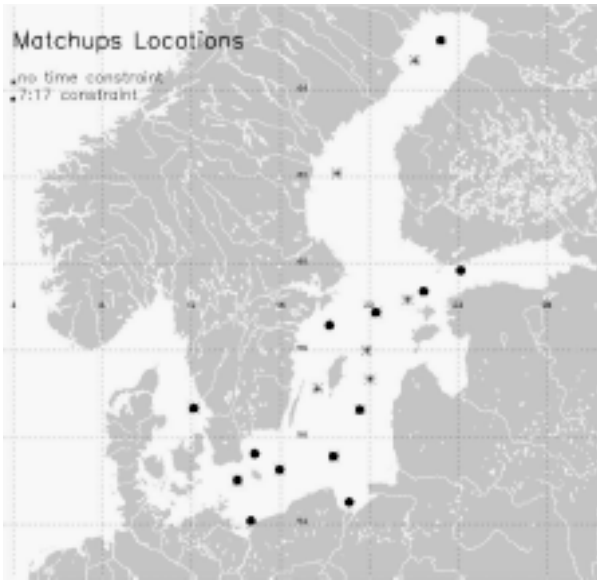

Fig. 4.8
Location of the match-ups displayed on Figures 4.5 and 4.6.
* indicate match-ups for which no time constraint was applied,
• are match-ups with a time difference between field and remote sensing values less than 5 hours.

Figure 4.8 shows the location of the match-ups that were retained for the analysis. Out of the 37 match-ups (Figure 4.5), 25 were obtained in 2000 and 12 in 2001, and equally distributed in spring, summer and autumn. As expected, there are almost no match-ups very close to the coastlines. In conclusion, the match-ups presented on Figures 4.5 and 4.6 are mostly from open water conditions.

4.3.3 Synoptic comparison

Even though the data body is quite large, the number of match-ups is relatively small for the 2 years considered. This is explained by several factors. First, the part of the field measurements that was collected during winter months or in very coastal areas is not suitable for comparison with remote sensing products. Then, SeaWiFS actually provides a view of a given area with a reasonable geometry of observation every other day. Finally, cloud coverage and various failures of the algorithms to produce valid outputs greatly reduce the basis for comparison.

To see if the results obtained with the match-ups scatter plots have any statistical representativity, Figure 4.9 shows the summer seasonal average (Jun.-Aug.) for 2000 obtained from remote sensing (*OC4v4*) and the composite map for that period obtained from the field measurements (this map is also seen on Figure 4.3). For the sake of comparison, the map obtained from the NASA Distributed Active Archive Center (DAAC-GSFC) is added. Since the two remote sensing products are based on the same bio-optical algorithm (*OC4v4* in that case), the differences must result mainly from the use of a different atmospheric correction scheme and secondarily from the quality checks enforced (flagging) and time binning procedures (e.g., treatment of outliers).

Depending on the area considered, agreements and discrepancies are noticed between the JRC seasonal map and the field measurement composite, both in terms of amplitude and gradients. It should be remembered that some abnormal features on the field data map might just be the results of one measurement point. The JRC product is consistently lower than the DAAC product, with the latter failing to reproduce the low ($1 mg.m^{-3}$) chlorophyll a concentrations in the southern Baltic. This comparison shows that no systematic underestimate or overestimate is discernible between field and remote sensing values (*OC4v4*-based).

To check if a systematic bias exists as far as the temporal variability is concerned, three areas in the Baltic Sea are considered (Figure 4.10). Those regions contain most of the match-ups (Figure 4.8). For each area, the average monthly JRC satellite (*OC4v4*-based) chlorophyll *a* concentration is computed and plotted as a function of time on Figure 4.10. The available field measurements located in those boxes are pooled together for every month and over-plotted together with the number of measurement points that make up the composite average. Those

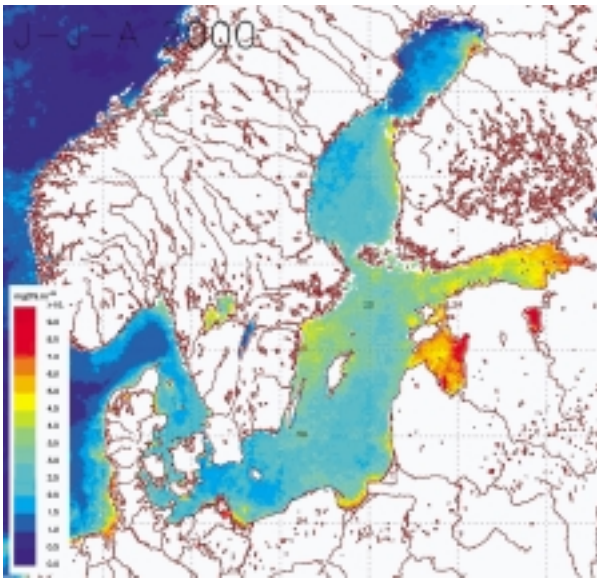

a)

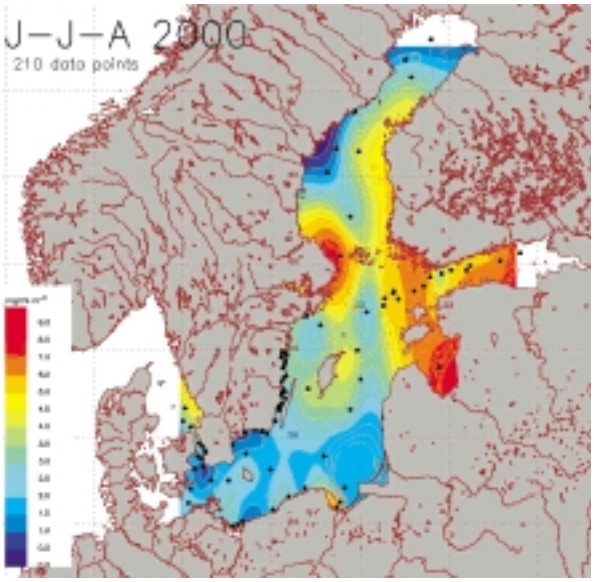

c)

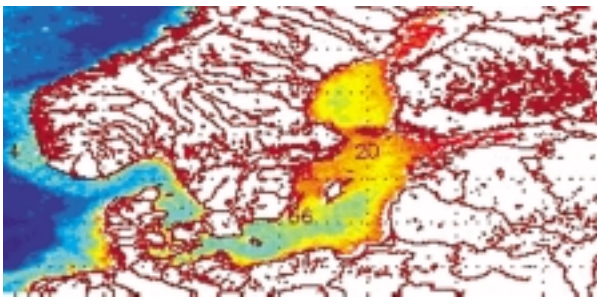

b)

Fig. 4.9
Seasonal average of chlorophyll a concentration computed with the OC4v4 algorithm as resulting ***a)*** from the JRC archive and ***b)*** from the DAAC. ***c)*** Composite of the field measurements available for summer 2000 with contouring procedure. The colour bar indicates the values 0, 0.5, 1, 1.5, 2, 2.5, 3, 3.5, 4, 4.5, 5, 6, 7, 8 and 9 mg.m^{-3}.

graphs show that there is no obvious bias between products, a view well in line with the results given by the match-ups analysis and the spatial comparison illustrated by Figure 4.9. It is stressed that the monthly field measurement averages are actually based on few measurement points (around 5). This figure completes Figure 4.2 and Table 4.1 since it indicates how many field measurements are available on a monthly basis for the regions outlined on the map (north, central and south).

4.3.4 Conclusion for match-up analysis

The analysis performed on selected match-ups has yielded poor results in terms of mean differences. Keeping only match-ups for which all 9 points of a 3x3-grid point square are valid satellite retrievals and the field measurement time is within 5 hours of the satellite overpass (15 match-ups), the differences between *in situ* and satellite values are actually reasonable (Figure 4.6). However, considering this number of match-ups or extra match-ups accepted with less stringent selection criteria, the correlation-between remote sensing products and *in situ* values is virtually nil, meaning that there is no statistical relationship between the two quantities.

Furthermore, for at least 3 out of 4 algorithms, the remote sensing values seem to be lower than the corresponding measurements. A broader view, in terms of spatial or temporal variability, does not indicate a systematic overestimate or underestimate of the satellite products (*OC4v4*-based) with respect to field measurements.

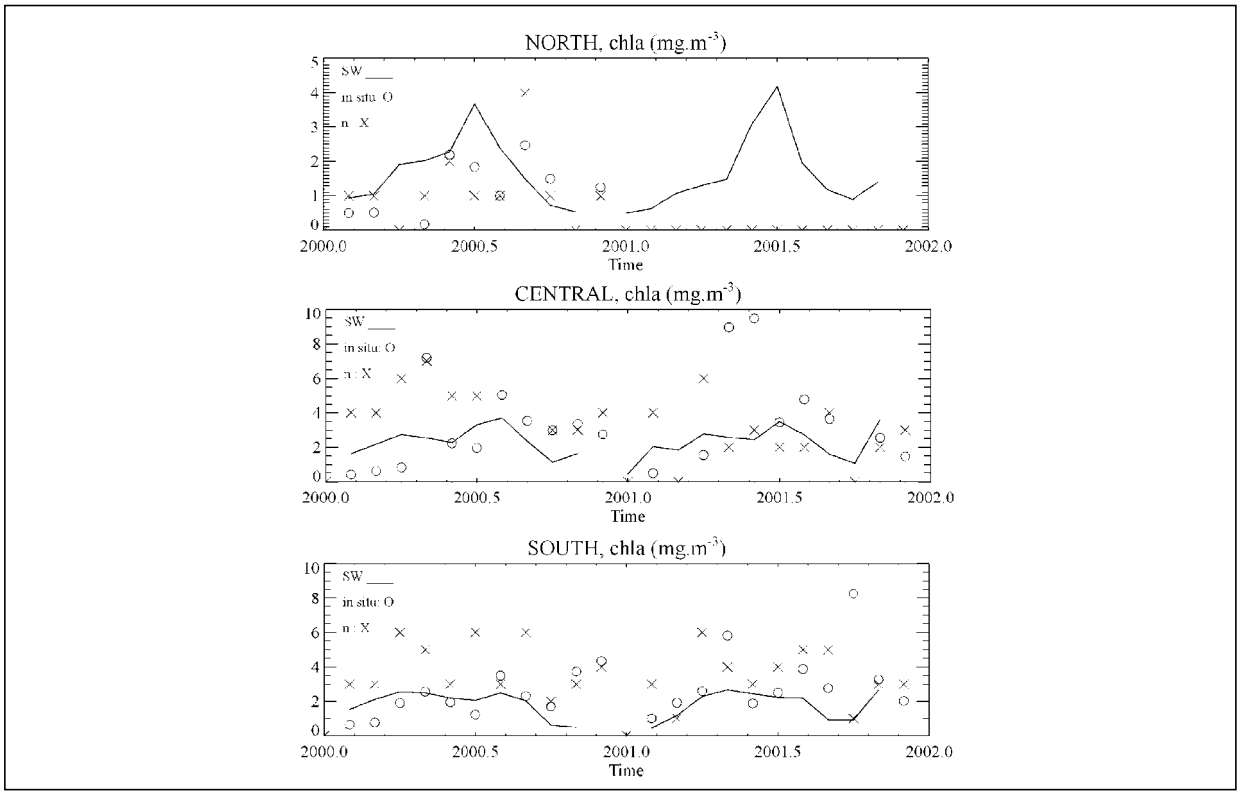

Fig. 4.10
Monthly values for the years 2000 and 2001 for the JRC *OC4v4* chlorophyll *a* concentration and the field measurement composite average for the 3 regions indicated on the map. The line is for satellite monthly values, O are the average values of all field measurements in a region for a given month, X is the number of the field measurements used to calculate this average (indicated with the same scale as the concentration, this number might be out of the graph). Notice the different scale between time series.

4.4 Transect lines

4.4.1 Presentation of the data set

Originally, 3 transects from the Alg@line project were provided by the Finnish Institute for Marine Research (FIMR) for comparison with satellite products. Those measurements are based on the operations of a flow-through fluorometer pumping water at a 5-m depth (Leppänen *et al.* 1995) during cruises crossing the basin between Travemünde and Helsinki. Subsequently, it appeared that the relationship between fluorometric measurements, taken in summer cruises, and actual chlorophyll *a* concentrations might not be straightforward and those measurements are not included in the comparison exercise with satellite data.

As a substitute, the FIMR provided discrete chlorophyll *a* measurements corresponding to Alg@line transects. The four transects represent a trip northward, starting late evening on the 4th July, 1st, 13th and 21st August 2001 and reaching Helsinki early morning less than 30 hours after departure (the transects therefore span 3 calendar days).

Taking into account the nature of those transects (consistent measurements taken across the basin on a 3-day period), it appeared preferable to consider each separately and make a comparison with the satellite maps produced over the 3 days of the transect (composite map). Such a procedure provides a more complete satellite data coverage representative of the basin-scale conditions encountered by the ship. Practically, there is thus no need to draw an arbitrary line between one day and the next for measurements taken in the middle of the night. Conversely, this procedure assumes a low synoptic day-to-day variability.

Figures 4.11a-d show the track of the ship with chlorophyll concentrations and dates of measurements over-plotted on the chlorophyll a average concentration estimated with *OC4v4* over the 3 days of the cruise. For the 4 transects, most concentrations are in the range 2-5 mg.m^{-3}.

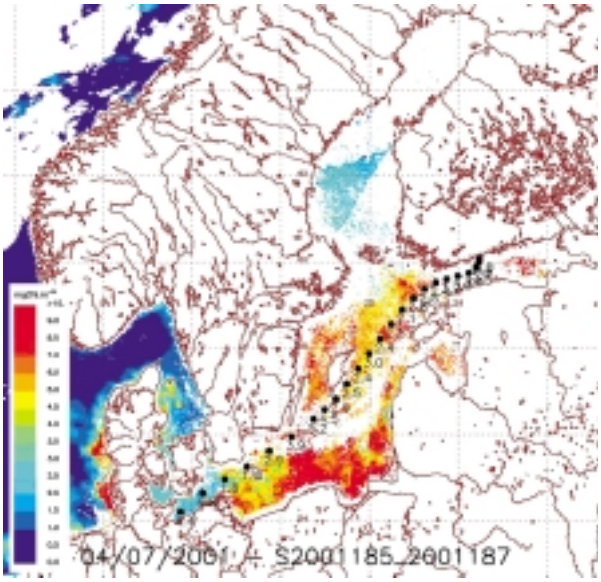

Fig. 4.11a
Three-day composite of the JRC *OC4v4* chlorophyll *a* concentration (4th-6th July 2001) with measurement points of the corresponding transect (date and concentration are indicated for each). The colour bar is as on Figure 4.9.

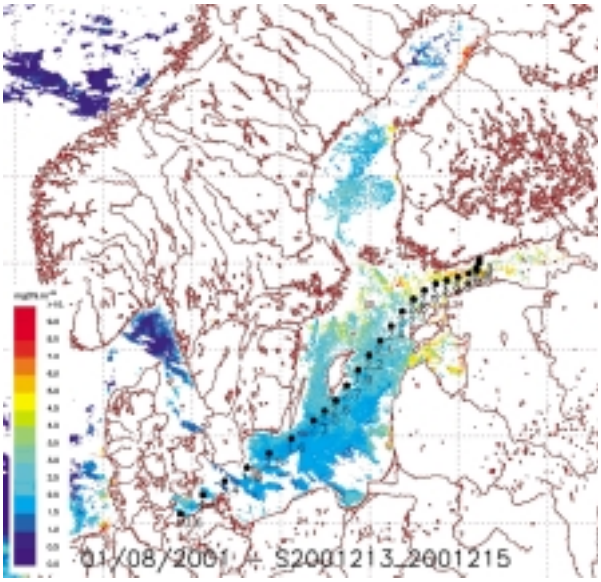

Fig. 4.11b
Three-day composite of the JRC *OC4v4* chlorophyll *a* concentration (1st-3rd August 2001) with measurement points of the corresponding transect (date and concentration are indicated for each). The colour bar is as on Figure 4.9.

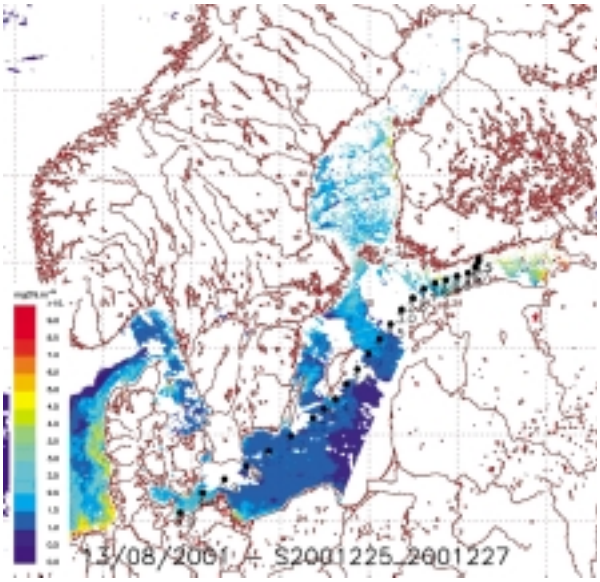

Fig. 4.11c
Three-day composite of the JRC *OC4v4* chlorophyll *a* concentration (13th-15th August 2001) with measurement points of the corresponding transect (date and concentration are indicated for each). The colour bar is as on Figure 4.9.

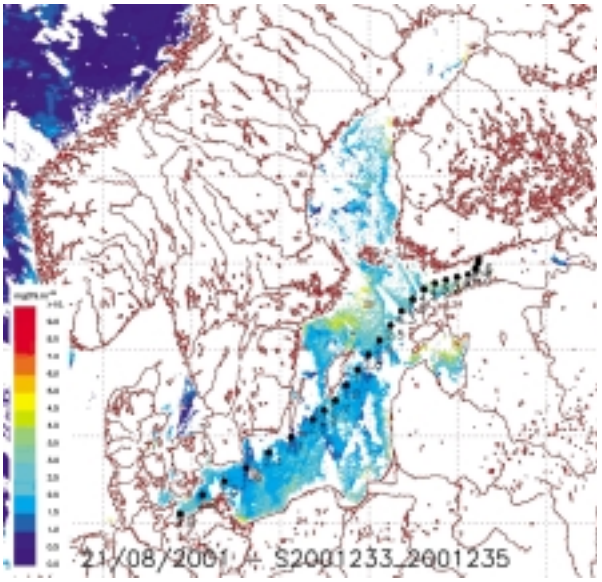

Fig. 4.11d
Three-day composite of the JRC *OC4v4* chlorophyll *a* concentration (21st-23rd August 2001) with measurement points of the corresponding transect (date and concentration are indicated for each). The colour bar is as on Figure 4.9.

4.4.2 Match-ups results

Similarly to the protocol defined in Section 3, the satellite products corresponding to the transect measurements were extracted for a 3x3-grid point square centered on the location of the measurement stations. In that section, the satellite products refer to the 3-day composites illustrated on Figure 4.11 and the results are presented for each transect. The 4 transects provide 3, 9, 10 and 7 match-ups for starting dates on 4th July, 1st, 13th and 21st August, respectively, and the results are shown on Figure 4.12a-d (notice the varying scales).

For the first transect, the remote sensing product *c1* underestimates the field values, *c2* is again characterized by a large scatter, *c3* gives an excellent comparison for 2 out of 3 points, and the *OC4v4* distribution is centered on the 1:1 line. Most of the match-up concentrations are between 2 and 3 mg m^{-3}.

For the second transect, the agreement between remote sensing and *in situ* concentrations is good for *c1* and *OC4v4* for 8 match-ups out of 9 displayed on Figure 4.12b. *c3* is characterized by relatively low values of the satellite-derived concentrations. One match-up features a concentration of 10.65 mg m^{-3} collected as first measurement at 10:30pm 1st August just after the departure of the ship, thus in a very coastal area.

The last two transects display match-ups for which the remote sensing values are again relatively lower than field values. For the latter transect, the agreement of *OC4v4* with respect to the *in situ* concentrations is reasonably good.

To conclude, the number of match-ups obtained with those 4 transects is quite remarkable (and fortunate). The differences observed between satellite and *in situ* values shown on Figure 4.12 are actually considered reasonable, particularly for the *OC4v4* algorithm. In any case, when associated with a coincident cloud-free image, the transects offer a good potential for basin-scale assessment of remote sensing products (e.g., Vepsäläinen *et al.* 2003).

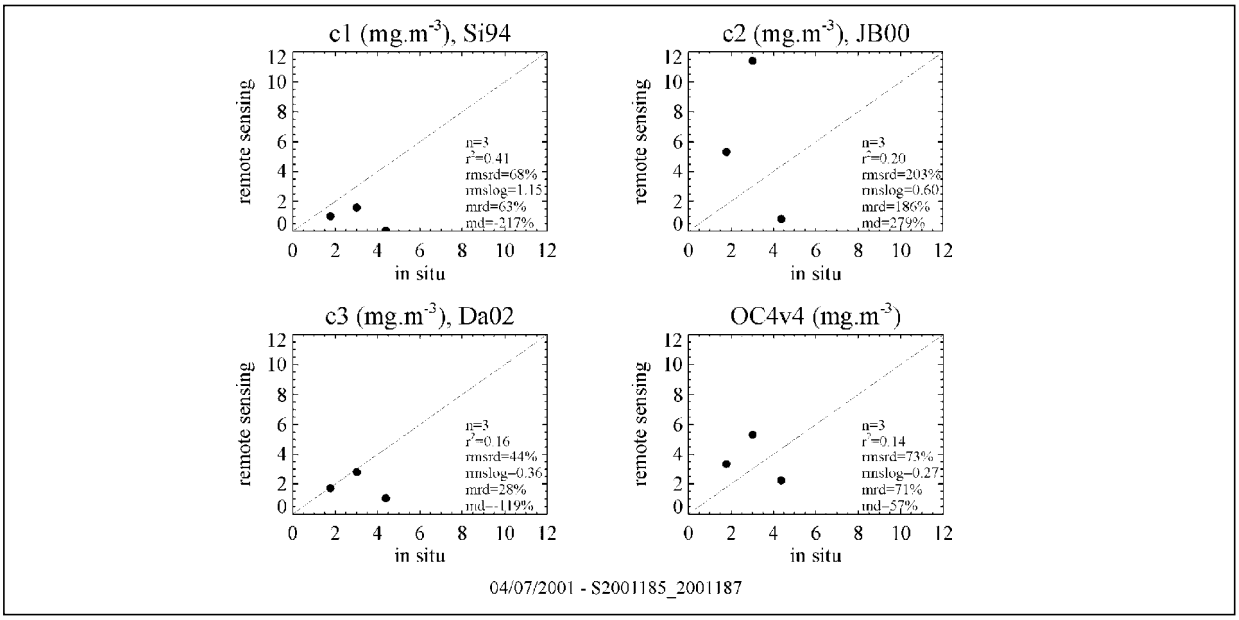

Fig. 4.12a
Match-ups between satellite derived and *in situ* chlorophyll *a* concentrations for the transect on 4th-6th July 2001. The number of valid points in the 3x3-grid point square centered on the measurement site is set to 9. *n* is the number of match-ups and the other variables were introduced in Section 4.2.

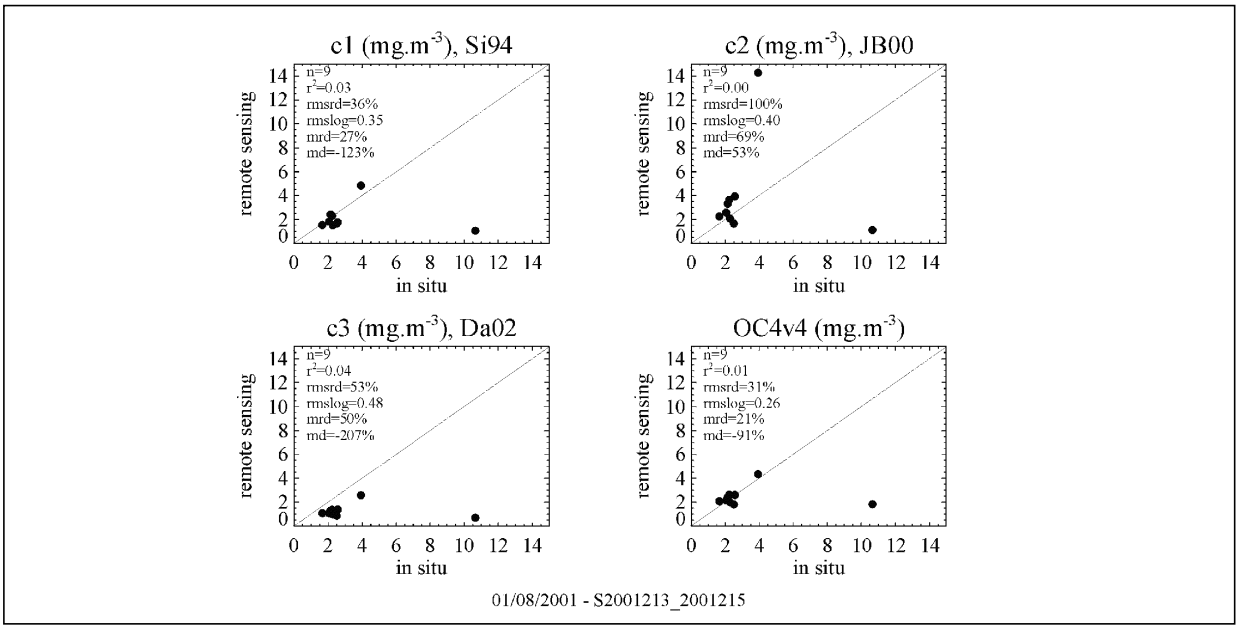

Fig. 4.12b
Match-ups between satellite derived and *in situ* chlorophyll *a* concentrations for the transect on 1st-3rd August 2001. The number of valid points in the 3x3-grid point square centered on the measurement site is set to 9. *n* is the number of match-ups and the other variables were introduced in Section 4.2.

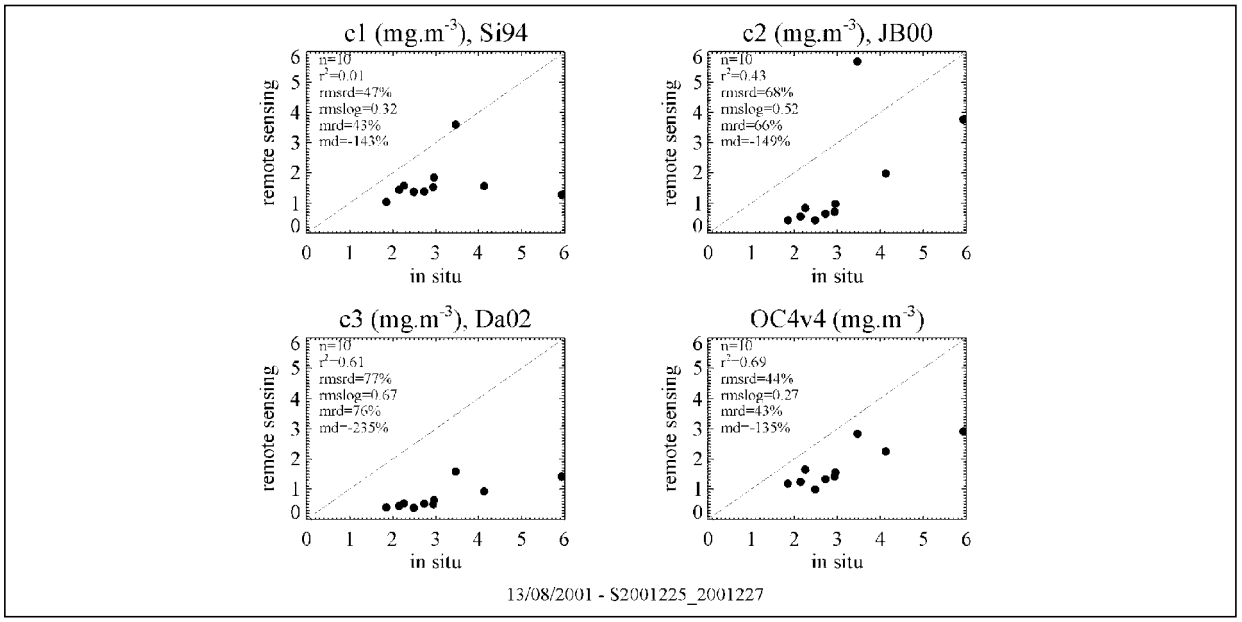

Fig. 4.12c
Match-ups between satellite derived and *in situ* chlorophyll *a* concentrations for the transect on 13th-15th August 2001. The number of valid points in the 3x3-grid point square centered on the measurement site is set to 9. *n* is the number of match-ups and the other variables were introduced in Section 4.2.

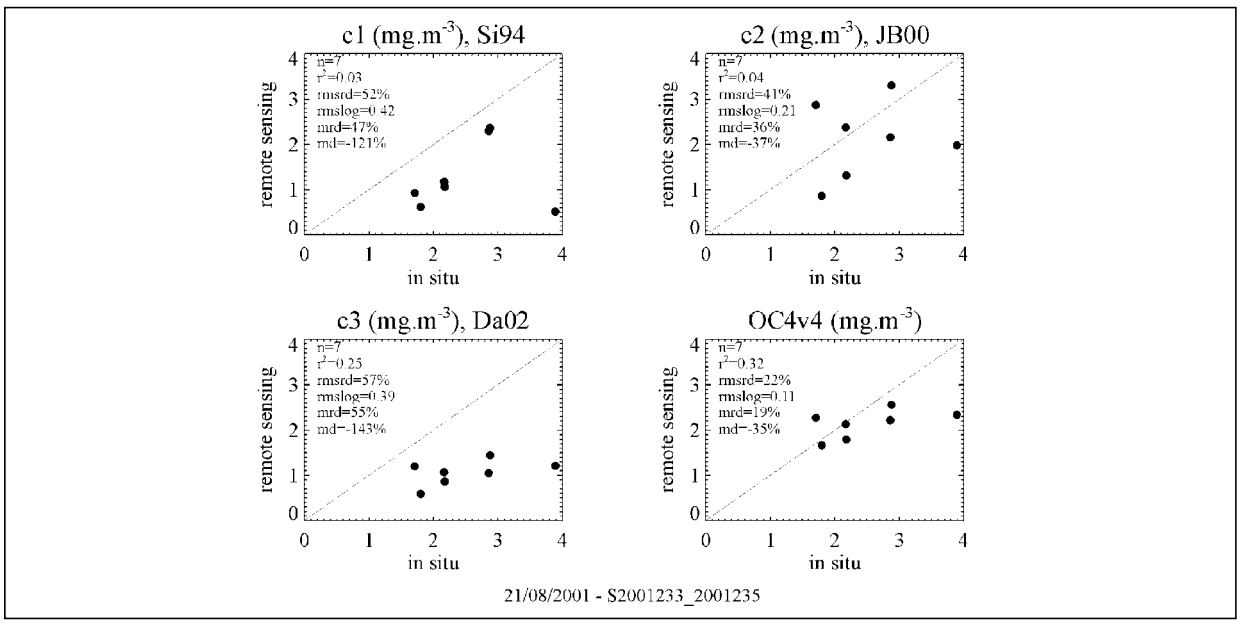

Fig. 4.12d
Match-ups between satellite derived and *in situ* chlorophyll *a* concentrations for the transect on 21st-23rd August 2001. The number of valid points in the 3x3-grid point square centered on the measurement site is set to 9. *n* is the number of match-ups and the other variables were introduced in Section 4.2.

4.5 Conclusions for algorithm comparison

Using data sets of chlorophyll *a* concentration profiles and single transects across the basin, uncertainties associated with remote sensing products calculated with four algorithms were assessed. Not surprisingly, the differences between satellite derived and *in situ* values were found to be large. An average underestimate of the satellite products with respect to the *in situ* concentrations is discernable, but no general bias is clearly shown. Compared with the results of Chapter 4.3 that presents a comparison based on measurements collected in various months and locations by different groups, it appears that none of the algorithms seems able to capture the overall variability of the chlorophyll *a* concentration. The comparison gives more encouraging results using match-ups obtained from separate Alg@line transects. In any case, it seems that the algorithms can not differentiate with a satisfactory level of accuracy the portion of the emerging light that is due to phytoplankton (and associate it with an actual pigment concentration) with respect to the other optical contributors (other particulate matter, chromophoric dissolved organic matter) found in the Baltic Sea (e.g., Ferrari *et al.* 1996, Højerslev *et al.* 1996, Kowalczuk 1999, Schwarz *et al.* 2002).

The algorithm *OC4v4* is often characterized by better statistics of comparison. Since it is an empirical algorithm whose formulation has been heavily conditioned by data collected in open ocean waters (O'Reilly *et al.* 2000), this result might seem surprising (even though a significant part of the development data set actually represents shelf and coastal waters). For various months and locations, the remote sensing reflectance spectra found in the Baltic Sea after atmospheric correction are not well represented in the SeaBAM data set that was used to construct the algorithm (D'Alimonte *et al.* 2003). Arguably, the statistical performance of *OC4v4* could be seen as fortuitous and resulting from a favourable functional form. On the other hand, it is worth remembering that the data that served for the definition of the other 3 algorithms are not necessarily highly representative of the spatio-temporal bio-optical variability found in the entire basin, because they are either based on a limited number of points or limited geographically (see Chapter 2).

Furthermore this comparison exercise does not give a precise indication of the performance of the different in-water empirical algorithms per se. The remote sensing product results from the system "calibration + atmospheric correction scheme + in-water algorithm", and the absence of optical data for the analysis precludes an estimate of the uncertainties associated with each compartment. Considering the maps on Figure 4.9 that shows *OC4v4*-based concentrations from two independent atmospheric correction schemes, the JRC processor produces relatively higher water- leaving radiances in the blue part of the spectrum. Whether this behaviour is valid can only be answered by a thorough validation of the atmospheric correction in Baltic waters, like that conducted in the North Adriatic (Mélin *et al.* 2003, see also Chapter 3).

In order to achieve this objective as well as to make any significant progress for remote sensing products, the availability of comprehensive atmospheric and bio-optical measurements accompanied by a sound modelling of the radiative transfer processes are necessary.

Acknowledgements

The author would like to thank Eija Rantajärvi and the Finnish Institute for Marine Research for the Alg@line transect data, Bertil Håkansson and the Swedish Meteorological and Hydrological Institute (SMHI) as well as the International Council for the Exploration of the Sea (ICES) for the availability of the chlorophyll data.

The SeaWiFS project (Code 970.2) and the Distributed Active Archive Center (Code 902) at the Goddard Space Flight Center, Greenbelt, MD20771, are thanked for the production and distribution of the SeaWiFS raw data, respectively.

5. Summary and recommendations

W. Schrimpf, G. Zibordi
European Commission – Joint Research Centre
Institute for Environment and Sustainability – Inland and Marine Waters Unit
I-21020 Ispra (VA), Italy

5.1 Summary

The project aimed at comparing, with respect to *in situ* values, the accuracy of existing empirical algorithms for the determination of chlorophyll *a* (*Chl a*) from SeaWiFS images of the Baltic.

Four algorithms were included in the exercise: three specifically developed for the Baltic Sea and a fourth algorithm proposed for global SeaWiFS products. The first Baltic algorithm was developed using *in situ* data of the German Baltic coastal area. The resulting empirical formula links optical field measurements and concentrations of chlorophyll *a* + phaeopigments. The second algorithm was developed using SeaWiFS reflectance data matching in situ *Chl a* measurements collected in the North Sea, Skagerrak and western Baltic Sea (the satellite data were processed with SeaDAS version 4.0, with an added module for turbid water correction). The third algorithm is based on field measurements of reflectance and *Chl a* collected in the Southern Baltic. The additional global algorithm is the *OC4v4* based on regressions performed on pairs of chlorophyll *a* concentrations and remote sensing reflectance measurements. Although its formulation was strongly influenced by measurements collected in open ocean waters, an appreciable part of the data was actually collected in shelf and coastal waters (but not in the Baltic area).

The atmospheric correction code applied for processing the SeaWiFS imagery used in the intercomparison exercise relies on the coupling of an approximate radiative transfer model and the vicarious calibration of the space sensor. The accuracy of the atmospheric correction scheme was formally assessed for atmospheric and water parameters typical of mid-latitude European sites, with specific reference to the North Adriatic Sea. The Baltic Sea is typically characterized by relatively high yellow substance absorption coefficients and solar zenith angles. It is then likely to expect that the accuracy of the proposed atmospheric correction scheme, when applied to Baltic Sea data, does not dramatically decrease for the aerosol optical thickness and ratios of remote sensing reflectance, but it could significantly decrease in the retrieval of the absolute water leaving radiance in the blue part of the spectrum. In this study the accuracy of SeaWiFS derived primary products of the Baltic Sea area was restricted to the aerosol products, because of the non-availability of *in situ* match-ups of normalized water leaving radiances. The accuracy analysis presented through scatter plots of SeaWiFS-derived versus *in situ* aerosol optical thickness at 443, 500, 670 and 865 nm, over 19 match-ups covering the period 2000-2001, shows a determination coefficient always higher than 0.90, and a mean relative percentage difference ranging between 14% and 18% for the different channels.

The uncertainties in the *Chl a* determined with the four algorithms considered was assessed using in situ *Chl a* from stations and transects across the basin. The mean relative percentage differences between satellite derived and *in situ* values are quite large, ranging from 45 to 101% on optimal intercomparison conditions (i.e., with a maximum five hour difference between in situ sampling and satellite overpass, and with an aggressive quality assurance of satellite data). An average underestimate of the satellite products with respect to the *in situ* concentrations is discernable, but no general bias clearly appears. Compared with the results that present a comparison based on measurements collected in various months and locations by different field groups, it appears that none of the algorithms captures the overall variability of the chlorophyll *a* concentration. The comparison gives slightly more encouraging results using match-ups obtained from separate Alg@line transects. But in general, it seems that the algorithms are not able to discriminate with a satisfactory level the spectral variations of emerging light due to phytoplankton (and associate it with an actual pigment concentration) with respect to those of the other optically significant components (i.e., dissolved organic

matter and total suspended matter). The best results are obtained with *OC4v4*. But considering that its formulation was heavily conditioned by data collected in open sea waters, the statistical performance of *OC4v4* could be seen as fortuitous and resulting from a favorable functional form. In any case, it is worth remembering that the data used for the development of the other regional algorithms are not necessarily highly representative of the spatial-temporal bio-optical variability found in the entire basin, because they are based on a limited number of points and restricted to specific regional areas.

Furthermore the remote sensing product results from the system "calibration + atmospheric correction scheme + in-water algorithm", and the absence of comprehensive optical data for the analysis precludes an estimate of the uncertainties associated with each compartment.

5.2 Recommendations

In view of the HELCOM monitoring and assessment tasks the Project should be considered as a first step towards a more routine use and application of *Chl a* satellite data. The comparison of *Chl a* algorithms proposed for the Baltic Sea highlighted *a)* quite large uncertainties associated with the use of the existing published empirical algorithms and *b)* once more the lack of comprehensive *in situ* measurements of apparent optical properties to satisfactorily support the validation of remote sensing products.

These general findings suggest:

1. the development of analytical or semi-analytical algorithms for the determination of optically significant components for the Baltic Sea, which are expected to overcome the limitations in accuracy of simple empirical algorithms based on remote sensing reflectance ratios;
2. the creation of an extensive (in time and space), comprehensive and accurate data set of the Baltic atmospheric, and marine inherent-apparent optical properties for algorithm development and successive product validation.

An optimal execution of the former tasks would require an international multi-year program effort involving atmospheric and marine bio-optical modellers (for model development and benchmarking), field scientists (for protocol definition, instrument inter-calibration and data collection), field data analysts (for the definition of common quality assurance methods and processing methods), data managers (to ensure archiving and distribution of data through standardized formats).

The performance of the Project revealed that there is significant remote sensing expertise and know-how available at institutions in 'HELCOM Countries'. It became obvious however that only combined efforts can lead to improved and harmonized products and their use in long-term marine monitoring and assessment activities. It is felt that a continuation and deepening of the collaboration started in the frame-

work of this Project would be very beneficial in regard to improving the capability of HELCOM Contracting Parties to use marine satellite remote sensing data and information for monitoring and assessment tasks. In terms of planning a HELCOM continuation project with a longer time horizon would be considered the appropriate framework to ensure and implement the collaboration. This Project should focus on:

- Co-operation and co-ordination of the 'individual' remote sensing activities in the Baltic Sea area in view of an operational use of satellites for monitoring and assessment purposes;
- Obtaining maximum synergy from the various ongoing remote sensing activities in Baltic Countries;
- Co-operating on the development and benchmarking of atmospheric and marine bio-optical models, field activities (protocol definition, instrument inter-calibration, data collection), data analysis (quality assurance) and data management;
- Producing joint products for HELCOM and EU ('Water Legislation') monitoring and assessment needs;
- Identifying research and development needs; joint efforts on the identified issues and preparing joint proposals for funding where appropriate.

References

Barnes, R.A., R.E. Eplee, G.M. Schmidt, F.S. Patt, C.R. McClain. Calibration of SeaWiFS. I. Direct techniques. *Appl. Opt*., 40, 6682-6700, 2001.

Bulgarelli B., V. Kisselev and L. Roberti. Radiative transfer in the atmosphere-ocean system: the finite element method. *Appl. Opt*., 38, 1530-1542, 1999.

Bulgarelli B. and F. Mélin. SeaWiFS data processing code REMBRANDT version 1.0 (Retrieval of Marine Biological Resources through Analysis of ocean colour DaTa). Code elements. *JRC Publication* EUR 19514 EN, 2000.

Bulgarelli B., G. Zibordi, F. Mélin. SeaWiFS data processing code REMBRANDT: Accuracy Evaluation of the Atmospheric Correction Method. *JRC Publication* EUR 20533 EN, 2003.

Bulgarelli B. and G. Zibordi. Remote sensing of ocean colour: accuracy assessment of an approximate atmospheric correction method", *Int. J. Remote Sens.*, 24, 491-509, 2003.

D'Alimonte, D., F. Mélin, G. Zibordi, J.-F. Berthon. Use of the novelty detection technique to identify the range of applicability of empirical ocean color algorithms. *IEEE Trans. Remote Sens. Geosci.*, 41, 2833-2843, 2003.

Darecki, M., S. Kaczmarek, J. Olszewski. SeaWiFS chlorophyll for the Southern Baltic. *Int. J. Remote Sens.*, in press, 2004.

Ferrari, G.M., M.D. Dowell, S. Grossi, C. Targa. Relationship between the optical properties of chromophoric dissolved organic matter and total concentration of dissolved organic carbon in the southern Baltic Sea region. *Mar. Chem*., 55, 299-316, 1996.

Højerslev, N.K., N. Holt, T. Aarup. Optical measurements in the North Sea – Baltic Sea transition zone. I. On the origin of the deep water in the Kattegat. *Cont. Shelf Res*., 16, 1329-1342, 1996.

Hooker, S.B., W. Esaias, G. Feldman, W. Gregg, C.R. McClain. An overview of SeaWiFS and ocean color. *NASA Tech. Memo.* 104566, S.B. Hooker and E.R. Firestone, Eds., 1, 1992.

Jørgensen, P.V., D.A.Berastegui: SeaWiFS data analysis in Danish waters: Chl-results compared to in situ values. Conference *Ocean from Space*, Venice 9th-13th October, 2000.

Kowalczuk, P.. Seasonal variability of yellow substance absorption in the surface layer of the Baltic Sea. *J. Geophys. Res*., 104, 30047-30058, 1999.

Leppänen, J.M., E. Rantajärvi. Unattended recording of phytoplankton and supplemental parameters on board merchant ships – an alternative to the conventional algal monitoring programs in the Baltic Sea. In *Harmful marine algal blooms*, pp. 719-724, Ed. P. Lassus, G. Arzul, E. Erard-Le Denn, P. Gentien, Marcaillore-Le Baut (Lavoisier, Paris), 1995.

Mélin, F., B. Bulgarelli, N. Gobron, B. Pinty, R. Tacchi. An integrated tool for SeaWiFS operational processing. *JRC Publication*, EUR 19576EN, 2000.

Mélin, F., C. Steinich, N. Gobron, B. Pinty, M.M. Verstraete. Optimal merging of LAC and GAC data from SeaWiFS. *Int. J. Remote Sens*., 23, 801-807, 2002.

Mélin, F., G. Zibordi, J.-F. Berthon. Assessment of atmospheric and marine SeaWiFS products for the North Adriatic Sea. *IEEE Trans. Remote Sens. Geosci*., 41, 548-558, 2003.

O'Reilly J.E., S. Maritorena, D.A. Siegel, M.C. O'Brien, D. Toole, B.G. Mitchell, M. Kahru, F.P. Chavez, P. Strutton, G.F. Cota, S.B. Hooker, C.R. McClain, K.L. Carder, F. Müller-Karger, L. Harding, A. Magnuson, D. Phinney, G.F. Moore, J. Aiken, K.R. Arrigo, R. Letelier, and M. Culver. Ocean color chlorophyll a algorithms for SeaWiFS, OC2, OC4: version 4. *NASA Tech. Memo*. 206892, S.B. Hooker and E.R. Firestone, Eds., 11, 9-23, 2000.

Ruddick, G., F. Ovidio, M. Rijkeboer. Atmospheric correction of SeaWiFS imagery for turbid coastal and inland waters. *Appl. Opt*., 39, 897-911, 2000.

Schwarz J.N., P. Kowalczuk, S. Kaczmarek, G.F. Costa, B.G. Mitchell, M. Kahru, F.P. Chavez, A. Cunningham, D. McKee, P. Gege, M. Kishino, D.A. Phinney, R. Raine. Two models for absorption by coloured dissolved organic matter (CDOM). *Oceanologia*, 44, 209-241, 2002.

Siegel, H., M.Gerth, M.Beckert. The variation of optical properties in the Baltic Sea and algorithms for the application of remote sensing data. *Ocean Optics XII, SPIE* vol. 2258, p. 894-905, 1994.

Sturm, B., G. Zibordi. Atmospheric correction of SeaWiFS data by an approximate model and vicarious calibration. *Int. J. Remote Sens.*, 23, 489-501, 2002.

Vepsäläinen, J.,T. Pyhälahti, E. Rantajärvi, K. Kallio, S. Pertola, T. Stipa, M. Kiirikki, J. Pulliainen, J. Seppälä, S. Koponen. The combined use of optical remote sensing data and unattended flow-through fluorometer measurements in the Baltic Sea. *Int. J. Remote Sens*., submitted, 2003.

Wang, M. The SeaWiFS atmospheric correction updates. *NASA Tech. Memo*. 206892, S.B. Hooker and E.R. Firestone, Eds., 9, 57-63, 2000.

Zibordi G., J.-F.Berthon, J.P. Doyle, S. Grossi, D. van der Linde, C. Targa, L. Alberotanza. Coastal Atmosphere and Sea Time Series (CoASTS): A long-term measurement program. *NASA Tech. Memo*. 206892, 19, S.B. Hooker and E.R. Firestone, Eds., 29 pp., 2002.

HELSINKI COMMISSION
Baltic Marine Environment Protection Commission

Katajanokanlaituri 6 B
FIN-00160 Helsinki
Finland

ISSN 0357-2994